

The theory of the measurement of magnetic multipole fields with rotating coil magnetometers

W.G. Davies

Nuclear Physics Branch, Chalk River Laboratories, K0J 1J0, Chalk River, Ontario, Canada

Received 29 July 1991

The theory of the measurement of multipole fields with rotating coil devices is developed with particular emphasis on the analysis of the sources of error in these measurements. The theory is developed in cylindrical coordinates for the full three-dimensional magnetic field. The presentation is quite detailed so that the reader can easily follow the development and, more importantly, adapt the results presented to his or her own requirements.

1. Introduction

Although there is a quite extensive literature [1–8] on the measurement of the magnetic fields of magneto-optical elements, used in beam transport systems and particle accelerators, there is no single, comprehensive treatment of the theory of rotating coil devices which includes the factors that limit their use for the accurate measurement of magnetic multipole fields. Lee–Whiting [1] has developed the basic theory of the measurement of quadrupole lens parameters, including the fringe-field region, in terms of a set of integrals that are related to the optical aberrations. Cobb and Cole [2], and Halbach [3,4], have related harmonic measurements of quadrupole and multipole lenses to possible errors in the construction and assembly of these devices. Hassenzahl [6] used the results of Halbach [3,4] to develop a method of reducing the duodecapole component in quadrupoles, which is now in common use. Green et al. [7] and Herrera et al. [8] have developed precision mapping machines which use the “radial” and “tangential” geometries, respectively. They have also taken quite different approaches to both the mechanical and electronic design, which have different strengths and weaknesses. The optimization of these machines is very difficult, and it is necessary to investigate at some breadth and depth the factors that limit the precision of the measurements.

This article will develop the theory of the measurement of multipole fields with rotating coil devices and in particular to analyze the sources of error in these measurements. The theory is developed for the full 3-dimensional magnetic field.

The following topics are covered:

1. Basic theory and notation,
2. The measurement of multipole parameters,
3. The tangential coil magnetometer.
4. Bucking coils,
5. Effect of finite coil size,
6. Effect of bowing of the coil,
7. Effect of torsional errors in the coil,
8. Effect of non-uniform angular velocity and angular vibrations,
9. Effect of errors in the integration of the signal,
10. Effect of radial vibrations of the coil,
11. Effect of coil sag under its own weight,

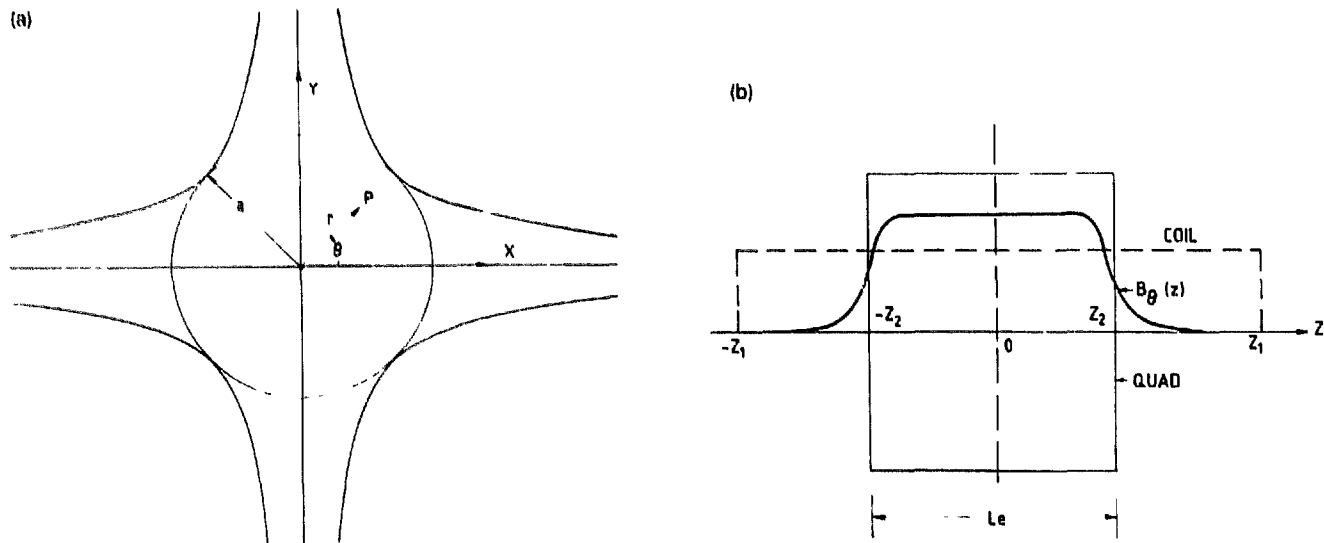


Fig. 1. (a) End view of a magnetic quadrupole lens showing the definition of the aperture radius, a , and the polar coordinates r and θ to any point, p , within the optically active volume, $r < a$, of the element. (b) Side view of the quadrupole showing the longitudinal, z , variation in the magnetic field. The origin of the coordinate system is assumed to be in the center of the element. The effective field boundaries (EFB) are assumed to be coincident with the physical ends of the element and indicated as $-z_2$ and $+z_2$. The effective length of the element is given by $L_e = 2z_2$. The points z_1 and $-z_1$ denote the ends of the measurement coil.

- 12. Effect of torsional vibrations in the coils,
- 13. Effect of eccentricity of the coil,
- 14. Errors specific to the tangential coil geometry,
- 15. Errors in the alignment of the bucking coils,
- 16. Radially misaligned apparatus,
- 17. Effects of non-linearities in the electronics.

The presentation of the theory developed here is quite detailed. This has been done to allow the reader to more easily follow the development and, more importantly, to adapt the results presented here to his/her own requirements.

2. Basic theory and notation

In the optically active volume of a dipole, quadrupole, or multipole magnet where no currents are present, we have that [9]

$$\mathbf{B} = -\nabla\Phi,$$
 (1)

where the magnetic scalar potential Φ satisfies the equation

$$\nabla^2\Phi = 0.$$
 (2)

It is most convenient to expand in cylindrical coordinates, as this describes both the geometry of the mapping machine and the magnetic elements that are mapped by such machines. Fig. 1 shows how the coordinate system is defined for a quadrupole lens; a similar definition would apply to other multipoles. In cylindrical coordinates eq. (2) becomes

$$\frac{1}{r} \frac{d}{dr} \left[r \frac{d\Phi}{dr} \right] + \frac{1}{r^2} \frac{d^2\Phi}{d\theta^2} + \frac{d^2\Phi}{dz^2} = 0$$
 (3)

Separation of variables in the usual way leads to

$$\Phi = R(r)\Theta(\theta)Z(z), \quad (4)$$

which in turn leads to three differential equations:

$$\frac{d^2 Z}{dz^2} + \nu^2 Z = 0, \quad (5)$$

$$\frac{d^2 \Theta}{d\theta^2} + n^2 \Theta = 0, \quad (6)$$

and

$$r^2 \left[\frac{d^2 R}{dr^2} \right] + r \frac{dR}{dr} - [\nu^2 r^2 + n^2] R = 0, \quad (7)$$

with general solutions

$$Z(z) = e^{i(\nu z + \gamma)}, \quad (8)$$

$$\Theta(\theta) = C_n e^{in\theta}, \quad (9)$$

and

$$R(r) = D_n(\nu) I_n(\nu r) + E_n(\nu) K_n(\nu r), \quad (10)$$

where I_n and K_n are modified Bessel functions [10]. Here we will use the complex form for the trigonometric functions because it greatly facilitates the analysis of most of the problems one encounters with these measurements, such as vibrations and mis-alignment. The results so derived can of course be reduced to the usual form using sin and cos whenever desired.

The solution for $Z(z)$ (eq. (8)) reduces to

$$Z(z) = \cos(\nu z + \gamma), \quad (11)$$

but we will retain the complex form of the solution for the reasons stated above. Furthermore, $Z(z) \rightarrow 0$ at least as rapidly as $1/z^2$ [1,2] (dipole field) as $z \rightarrow \pm\infty$. If the lens is symmetric about $z = 0$ then $\gamma = 0$. The boundary conditions put no restriction on ν . Hence all real values of ν are allowed.

The boundary condition that Φ be single valued and reflect the periodicity of the device implies that n is an integer:

$$|n| = 2p + 1, \quad (p = 0, 1, 2, \dots), \quad (12)$$

for a dipole ^{#1},

$$|n| = 4p + 2, \quad (13)$$

for a quadrupole, and

$$|n| = N(p + \frac{1}{2}), \quad (14)$$

for any lens of multipolarity N . Finally, the condition that $\Phi(r, \theta, z)$ be finite at $r = 0$ implies that $E_n = 0$.

Hence the general solution becomes

$$\Phi(r, \theta, z) = \sum_n \int_{-\infty}^{\infty} I_{|n|}(|\nu| r) A_n(\nu) e^{in\theta} e^{i\nu z} d\nu, \quad (15)$$

^{#1} It is only meaningful to use a device of this type in "straight" dipoles.

where $A_n(\nu) = C_n D_n(\nu)$. Here, the sum over n includes both positive and negative values, and for Φ to be real, the coefficients A_n must be such that $A_{-n}^*(-\nu) = A_n(\nu)$, where $*$ means complex conjugate. At any fixed radius $r = a$, $\Phi(a, \theta, z)$ can be expanded in the Fourier series

$$\Phi(a, \theta, z) = \sum_{n=-\infty}^{\infty} U_n(z) e^{in\theta}, \quad (16)$$

where

$$U_n(z) = \int_{-\infty}^{\infty} F_n(\nu) e^{i\nu z} d\nu, \quad (17)$$

and

$$F_n(\nu) = \frac{1}{2\pi} \int_{-\infty}^{\infty} U_n(z) e^{-i\nu z} dz. \quad (18)$$

For $\Phi(a, \theta, z)$ to be real, $U_{-n}^* = U_n$ which implies that $F_{-n}^*(-\nu) = F_n(\nu)$. From a comparison of eqs. (15) and (17), we see that

$$A_n(\nu) = F_n(\nu)/I_{|n|}(|\nu|a). \quad (19)$$

Although a can be any fixed radius where eq. (1) holds, let us define it to be the aperture radius of the device. If we replace $I_n(\nu r)$ by its power series expansion [10]

$$I_n(\nu r) = \left(\frac{\nu r}{2}\right)^n \sum_{m=0}^{\infty} \frac{1}{m!(n+m)!} \left(\frac{\nu r}{2}\right)^{2m}, \quad (20)$$

in eqs. (19) and (15), we find that

$$\Phi(r, \theta, z) = \sum_n \sum_{m=0}^{\infty} k_{nm}(z) \left(\frac{r}{a}\right)^{|n|+2m} e^{in\theta}, \quad (21)$$

where

$$k_{nm}(z) = \frac{a^{2m}}{m!(|n|+m)!} \int_{-\infty}^{\infty} W_{nm}(\nu) e^{i\nu z} d\nu, \quad (22)$$

$$W_{nm}(\nu) = F_n(\nu) \left[\frac{\nu}{2}\right]^{2m} \left\{ \sum_{l=0}^{\infty} \frac{1}{l!(|n|+l)!} \left[\frac{\nu a}{2}\right]^{2l} \right\}^{-1}. \quad (23)$$

The sum over m , from the expansion of the Bessel function, comes from the end-effects or fringe-field region of the device. The $m=1$ term has the same radial dependence on the field as the $n+2$ pole term, i.e. for quadrupole elements it generates an octupole-like radial dependence in Φ that has quadrupole symmetry, and so on. The first few values of $k_{nm}(z)$ are shown in fig. 2 for a quadrupole lens.

From eqs. (15), (19) and (20), we can derive the following useful recursion formula [1]

$$k_{nm}(z) = \frac{(-1)^m |n|! a^{2m}}{2^{2m} m!(|n|+m)!} \frac{d^{2m}}{dz^{2m}} [k_{n0}(z)], \quad (24)$$

The transverse components of the magnetic field \mathbf{B} are, from eq. (21)

$$B_r = -\frac{\partial \Phi}{\partial r} = -\frac{1}{a} \sum_n \sum_{m=0}^{\infty} (N+2m) e^{in\theta} k_{nm}(z) \left(\frac{r}{a}\right)^{N+2m-1}, \quad (25)$$

$$B_\theta = -\frac{1}{r} \frac{\partial \Phi}{\partial \theta} = -\frac{i}{a} \sum_n N e^{in\theta} \sum_{m=0}^{\infty} k_{nm}(z) \left(\frac{r}{a}\right)^{N+2m-1}, \quad (26)$$

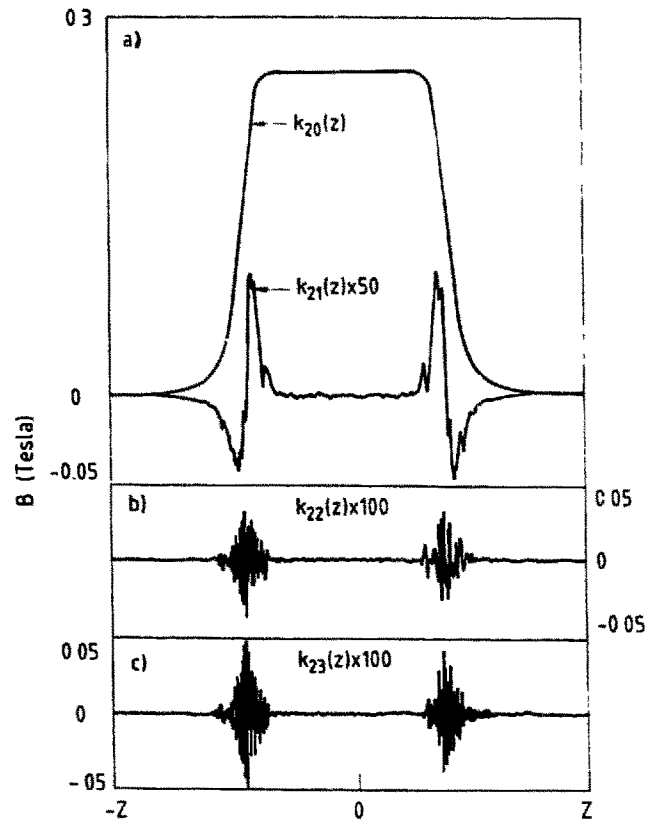


Fig. 2. Plot of k_{20} , $50k_{21}$, $100k_{22}$, and $100k_{23}$ compared with the Σk_{2m} . For this particular geometry ($a = 26$ mm, $L = 330$ mm), k_{20} is indistinguishable from Σk_{2m} on the scale of this plot. Hence for this geometry, the field is dominated by k_{20} and the contribution from the higher harmonics of the fringe-field are quite small. For elements where the aperture/length ratio is larger, the $m > 0$ terms grow very rapidly.

where we adopt the convention that $N \equiv |n|$. In many applications, it is convenient to know the “bending power” of a dipole,

$$B_l = \int_{-\infty}^{\infty} B \, dz, \quad (27)$$

or the focusing power of a quadrupole

$$P = \int g \, dz, \quad (28)$$

where the field gradient g is

$$g = \frac{\partial B}{\partial r}. \quad (29)$$

The bending and focusing powers are readily obtained from

$$\Phi_l = \int \Phi \, dz. \quad (30)$$

If we substitute eq. (15) into eq. (30) and interchange the order of integration in eq. (15), we can perform the integration over z , which leads to

$$\int_{-\infty}^{\infty} e^{i\nu z} \, dz = 2\pi\delta(\nu), \quad (31)$$

for constant r ; $\delta(\nu)$ is the Dirac δ -function. Finally, if we substitute eq. (31) into eqs. (22) and (23) and integrate over ν , we find that all terms with $m > 0$ vanish, and eq. (30) becomes

$$\Phi_l(r, \theta) = \sum_n K_n \left(\frac{r}{a} \right)^N e^{im\theta}, \quad (32)$$

where

$$K_n = \int_{-\infty}^{\infty} k_{n0}(z) dz. \quad (33)$$

Thus, although Φ and B contain a larger number of “higher harmonics” coming from the fringe-field via the Bessel function, these harmonics integrate to zero in Φ_l , B_l , and P and, in fact, along all trajectories for which $r = \text{constant}$. The “Bessel terms” r^{2m} are not easy to measure because they have the symmetry of the Fourier terms on which they are based. Clearly these terms are unimportant for sufficiently weak lenses where the particle trajectories follow orbits of nearly constant r . They are not negligible for strong lenses.

3. Measurement of the multipole parameters

The voltage generated by a generalized loop of wire [1] is

$$\mathcal{E} = - \int_{-z_1}^{z_1} dz \int_0^{F(z)} \left[\frac{dB_\theta}{dt} \right] dr, \quad (34)$$

where B_θ is given by eq. (26) and $F(z)$ describes the shape of the wire loop which for convenience is assumed to lie in a plane with one arm on the axis of rotation. If we have a rectangular loop then $F(z) = c = \text{constant}$ for z between $-z_1$ and z_1 . We will refer to such a loop as the “radial” geometry. If we assume that the loop includes “all” of the flux, as shown in fig. 1, then we can replace $\pm z_1$ by $\pm\infty$. On integrating over z , we obtain from eqs. (26) and (34) that

$$B_{l_n} = \int_{-z_1}^{z_1} B_\theta dz = -\frac{1}{a} \sum_n n K_n \left(\frac{r}{a} \right)^{N-1} e^{im\theta}. \quad (35)$$

Hence eq. (34) becomes for the rectangular loop

$$\mathcal{E} = -\omega \int_0^c \frac{dB_{l_\theta}}{d\theta} dr, \quad (36)$$

where

$$\frac{dB_{l_\theta}}{dt} = \omega \frac{dB_{l_\theta}}{d\theta}, \quad (37)$$

and we assume that the angular frequency ω is constant (note $\theta = \omega t$). On substitution of eq. (35) into eq. (36) we obtain after performing the integration over r :

$$\mathcal{E} = -\omega \sum_n N K_n \left(\frac{c}{a} \right)^N e^{im\theta}. \quad (38)$$

Thus the voltage generated by a rectangular loop that includes all of the flux provides no information about the “Bessel” terms r^{2m} . It can be shown [11] that eq. (38) also holds for a rectangular loop that “integrates” over only one fringe-field region as long as $[dk_{nm}(z)/dz] = 0$ at the end points. In order to measure these terms [1] it is necessary to use a loop in which $r = F(z)$ is not constant. The simplest coil

to treat mathematically is a pair of triangular loops extending from $z = 0$ to $\pm z_1$ where $B \approx 0$ and $F(\pm z_1) = a$. The EMF is found by substituting eq. (26) into eq. (34) with

$$F(z) = \begin{cases} \frac{a|z|}{z_1}; & 0 < z < |z_1|, \\ 0; & z > |z_1|, \end{cases} \quad (39)$$

and integrating first with respect to r . The result is

$$\int_0^{F(z)} \frac{dB_\theta}{dt} dr = \omega \sum_n e^{in\theta} \sum_{m=0}^{\infty} \frac{n^2}{(N+2m)} k_{nm}(z) \left[\frac{z}{z_1} \right]^{N+2m}. \quad (40)$$

If we substitute eq. (22) into (40) and retain only those factors that involve z , the integration over z can be written in the form:

$$\int_{-z_1}^{z_1} \dots dz = 2 \int_0^{z_1} \left[\frac{z}{z_1} \right]^{N+2m} e^{wz} dz = \frac{z_1}{p} \{ \mathcal{M}(p, p+1, i\xi) + \mathcal{M}(p, p+1, -i\xi) \}, \quad (41)$$

where $p = N + 2m + 1$, $\xi = z_1 \nu$ and \mathcal{M} is a confluent hypergeometric function [10]; we have used solution (11) for $Z(z)$. For small ξ , eq. (41) reduces to

$$2 \frac{z_1}{p} \left[1 - \frac{p}{p+2} \frac{\xi^2}{2!} + \dots \right] \rightarrow 2 \frac{z_1}{p} \cos(\xi), \quad (42)$$

if p is sufficiently large. As $\xi \rightarrow \infty$, eq. (41) becomes

$$z_1 \sin(\xi), \quad (43)$$

which is independent of p . Hence, if we substitute eq. (41) back into eq. (34), the EMF generated by the triangular loop can be written

$$\begin{aligned} \mathcal{E} = & -\omega \frac{z_1}{a} \sum_n e^{in\theta} \sum_{m=0}^{\infty} \frac{n^2}{p(p-1)} \frac{a^{2m}}{m!(N+m)!} \\ & \times \int_{-\infty}^{\infty} W_{nm}(\nu) \{ \mathcal{M}(p, p+1, i\xi) + \mathcal{M}(p, p+1, -i\xi) \} d\nu. \end{aligned} \quad (44)$$

The factor $W_{nm}(\nu)$ (eq. (22)) is clearly an even function of ν if $F_n(\nu)$ is even; F_n must be even from the boundary conditions on eqs. (8) and (44). The EMF (eq. (44)) is also clearly a function of m since W and \mathcal{M} are both non-vanishing over a wide range of values of m , p and ν . The integral in eq. (44) has been evaluated algebraically by Lee-Whiting [1] for a pure quadrupole field.

3.1. Integration of the EMF

In the previous section, we have assumed that the angular frequency is constant. This is usually not the case (see section 4.4 for a discussion of non-uniform angular frequency). This problem is alleviated but not completely overcome by integrating the EMF produced by the coil (see sections 4.4 and 4.5). For convenience, we assume a radial coil that encloses ‘‘all’’ of the flux. One revolution of the coil is divided into a set of equally spaced angular intervals of width $2\delta\theta$. First, we reorder the operations of integration and differentiation in eq. (34) and obtain:

$$\mathcal{E} = -i \frac{d}{dt} \sum_n \frac{n}{N} K_n \left(\frac{c}{a} \right)^N e^{in\theta(t)}. \quad (45)$$

where we explicitly indicate that θ is some unspecified function of t . Hence

$$Q = \int_{t-\Delta t}^{t+\Delta t} \mathcal{E} \, dt = -i \sum_n \frac{n}{N} K_n \left(\frac{c}{a} \right)^N \{ e^{in\theta(t+\Delta t)} - e^{in\theta(t-\Delta t)} \}. \tag{46}$$

We see from eq. (46) that the integrated voltage Q is independent of the angular frequency ω . The value of Q (webers) is well defined as long as $\theta(t)$ is smooth enough that the angle encoder behaves correctly. For sufficiently large amplitude “high” frequency vibrations this may in fact not be the case (see section 4.4). In an integrating system, the angle θ will be measured directly, and we need not know the values of t and δt that correspond to this angle. Hence we can replace $\theta(t + \delta t)$ and $\theta(t - \delta t)$ by the angles $\theta + \delta\theta$ and $\theta - \delta\theta$ which if substituted into eq. (46) leads to

$$Q = i \sum_n \frac{n}{N} K_n \left(\frac{c}{a} \right)^N e^{in\theta} \{ e^{in\delta\theta} - e^{-in\delta\theta} \} = -2 \sum_n \frac{n}{N} K_n \left(\frac{c}{a} \right)^N e^{in\theta} \sin(n\delta\theta) \tag{47}$$

Note: the integration “bin” width is $2\delta\theta$.

3.2. The tangential coil

Another coil geometry that has certain advantages for some types of measurements is the “Tangential Coil” arrangement [8], shown in fig. 3. The EMF generated by the two arms of the tangential coil can be written immediately from eq. (38) as:

$$\mathcal{E} = -\omega \sum_n N K_n \left(\frac{c}{a} \right)^N \{ e^{in(\theta+\Omega/2)} - e^{in(\theta-\Omega/2)} \} = -2i\omega \sum_n N K_n \left(\frac{c}{a} \right)^N e^{in\theta} \sin\left(n\frac{\Omega}{2}\right), \tag{48}$$

where Ω is the tangential opening angle of the coil (see fig. 3). The sensitivity to any harmonic is now a more complex function of n than with the simple rectangular coil. The maximum signal strength is twice that given by eq. (38) when $\Omega = \pi/N$, which is to be expected as we are adding the signals from the two wires. However, in general the signal is attenuated by the factor $\sin(n\Omega/2)$ when $n\Omega \neq \pi$ so that the

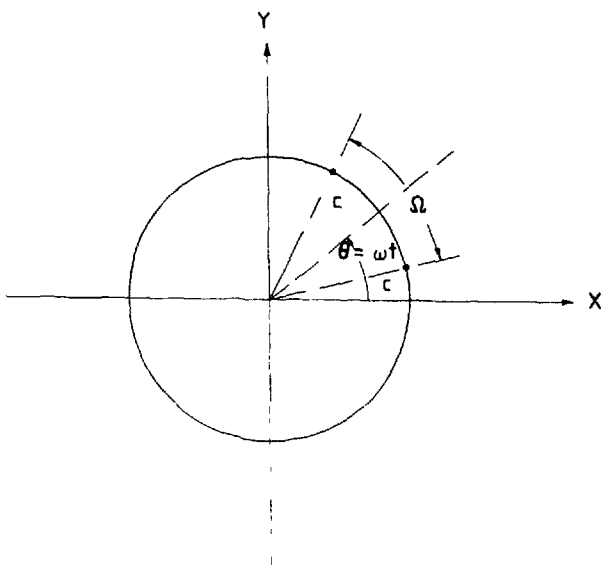


Fig. 3 Tangential coil geometry. The radius, c , to the coil center are indicated along with the definition of the opening angle Ω . The polar (rotation) angle θ is defined as the angle to the bisector of the coil

choice between a tangential or a radial coil depends upon the types of measurements required. This attenuation can be an advantage in certain circumstances where the suppression of harmonics very different from the “design” or optimum value is desired (except for $\Omega = \pi/2$). We should also note that eq. (48) is phase shifted by $\pi/2$ with respect to the result of eq. (38). This is equivalent to a measurement of B , which might be expected as the wire loop has been rotated by 90° with respect to the radial geometry.

3.3. Bucking coils

If one is primarily interested in accurate measurements of harmonics other than the fundamental, it is very advantageous to “buck” out the fundamental harmonic, which can often be more than 1000 times stronger than the other terms. Also, as we shall see during the discussion of mechanical vibrations, bucking reduces dramatically the vibrational coupling of the fundamental to the other harmonics. If we assume for convenience a radial coil with radius c_1 and a bucking coil with radius c_2 , azimuthally aligned with the main coil, we obtain immediately from eq. (38) that

$$\begin{aligned} \mathcal{E} &= -\omega \left\{ \sum_n NK_n \left(\frac{c_1}{a} \right)^n e^{in\theta} - \sum_n NK_n \left[\frac{c_1}{c_2} \right]^n \left(\frac{c_2}{a} \right)^n e^{in\theta} \right\} \\ &= -\omega \sum_n NK_n \left\{ \left(\frac{c_1}{a} \right)^n - \left[\frac{c_1}{c_2} \right]^n \left(\frac{c_2}{a} \right)^n \right\} e^{in\theta}, \end{aligned} \quad (49)$$

where n is the harmonic that is to be “bucked out”; $[c_1/c_2]^n$ is a constant. One generally uses the turns ratio of the coils or an electronic network to get the factor $(c_1/c_2)^n$. For the tangential geometry, the bucking coil usually has radius c_1 , but a different opening angle Ω_B . The bucking constant is given by $C_n = \sin(n\Omega/2)/\sin(n\Omega_B/2)$. The harmonics adjacent to the fundamental are attenuated by bucking, but this is more than compensated by the fact that the gain of the amplifiers can be two or three orders of magnitude greater. Hence the resolution of the device is greatly improved.

4. Errors and effects that limit the accuracy of the measurements

There are many factors that limit the accuracy of the measurements. The most important of these will be discussed in this section. In general the theory will be developed for the simple rectangular or radial coil, but the results are usually immediately applicable to the tangential coil and to bucked systems. Where there are extra factors applicable to tangential coil and bucked geometries, these will be noted explicitly

4.1. Effect of the finite size of the coil

Let us assume a uniform winding density, d_1 per unit area, such that the total number of turns N_1 is

$$N_1 = d_1 \int_{c-\Delta r}^{c+\Delta r} r \, dr \int_{\theta-\Delta\theta}^{\theta+\Delta\theta} d\theta' = 4d_1 c \, \Delta r \, \Delta\theta. \quad (50)$$

The EMF generated by a coil of finite dimensions is found by integrating eq. (38) over the area of the coil and leads to

$$\mathcal{E} = -2\omega a c d_1 \sum_n \frac{NK_n}{(N+1)} \left[\left(\frac{c+\Delta r}{a} \right)^{N+1} - \left(\frac{c-\Delta r}{a} \right)^{N+1} \right] \left[\frac{e^{in(\theta+\Delta\theta)} - e^{in(\theta-\Delta\theta)}}{2in} \right], \quad (51)$$

which reduces to

$$\mathcal{E} = -2\omega a c d_i \sum_n \frac{N K_n}{(N+1)} \left[\left(\frac{c + \Delta r}{a} \right)^{N+1} - \left(\frac{c - \Delta r}{a} \right)^{N+1} \right] e^{in\theta} \frac{\sin(n \Delta \theta)}{n}, \quad (52)$$

when we reduce the trigonometric integral in eq. (51) as in eq. (48). If we assume that the size of the coil is small, then we can expand the radial factors in a binomial series and retain only the first few terms. The result is

$$\begin{aligned} \mathcal{E} = & -4\omega d_i a c \sum_n \frac{N K_n}{(N+1)} \left[\binom{N+1}{1} \left(\frac{c}{a} \right)^N \left(\frac{\Delta r}{a} \right) + \binom{N+1}{3} \left(\frac{c}{a} \right)^{N-2} \left(\frac{\Delta r}{a} \right)^3 + \dots \right] \\ & \times \left\{ \Delta \theta - \frac{n^2 \Delta \theta^3}{6} + \dots \right\} e^{in\theta}, \end{aligned} \quad (53)$$

where we have also expanded the factor $\sin n\Delta\theta$, shown in $\{\dots\}$. If we factor out $\Delta\theta(\Delta r/a)$ and make a further reduction of the binomial we obtain

$$\mathcal{E} = -N_i \omega \sum_n N K_n \left(\frac{c}{a} \right)^N \left[1 + \frac{N(N-1)}{6} \left(\frac{c}{a} \right)^{-2} \left(\frac{\Delta r}{a} \right)^2 + \dots \right] \left\{ 1 - \frac{n^2 \Delta \theta^2}{6} + \dots \right\} e^{in\theta}, \quad (54)$$

where we have made use of the fact that $N_i = 4d_i a c \Delta\theta(\Delta r/a)$.

We see from eq. (54) that the two second-order terms nearly cancel for large n if the coil is “square”. We can, of course, make this cancellation exact for any given $n > 1$ by setting

$$\Delta r = c \Delta \theta \sqrt{\frac{N}{N-1}}. \quad (55)$$

This analysis assumes a “wedge” shaped coil, but if the dimensions are sufficiently small the error incurred by using a rectangular or square coil will be negligible. In fact there is no error to any order introduced by a circular coil of uniform winding density [12]. This may be proved by applying the expansion of section 4.11 for the coil and integrating over its area.

4.2. Effects of a z-dependent radial error in the coil

Let us investigate the effects of a radially dependent deformation of a radial coil that could arise from warping, bowing, taper, or misalignment of the coil. For simplicity, let us expand the errors about $z = 0$, which is assumed to be in the center of the element as follows:

$$F(z) = c + \sum_{p=1} b_p z^p \quad (56)$$

where we assume that any constant term is already included in c . On substitution of eq. (26) into eq. (34), we obtain:

$$\mathcal{E} = -\omega \int_{-\infty}^{\infty} dz \int_0^{c+b_p z^p} dr \sum_n \frac{n^2}{a} e^{in\theta} \sum_{m=0}^{\infty} k_{nm}(z) \left(\frac{r}{a} \right)^{N+2m-1}, \quad (57)$$

where the upper limit of integration is a single general term in eq. (56). If we perform the integral over r in eq. (57) and expand the result in a binomial series as in eq. (52), we obtain the following integral over z .

$$\int_I \dots dz = \int \left\{ 1 + M \left(\frac{b_p z^p}{c} \right) + \frac{M(M-1)}{2!} \left(\frac{b_p z^p}{c} \right)^2 + \dots \right\} k_{nm}(z) dz, \quad (58)$$

where $M = (N + 2m)$. The first term in eq. (58) is just K_n by virtue of eq. (33). The second term in eq. (58) yields:

$$\int_{II} = \frac{Mb_p}{c} \begin{cases} 0; & \text{if } p \text{ is odd,} \\ \int z^p k_{nm}(z) dz; & \text{for } p \text{ even and } \neq 0, \\ K_n; & \text{for } p = 0, \end{cases} \quad (59)$$

and the third term yields

$$\int_{III} = \frac{M(M-1)}{2!} \left[\frac{b_p}{c} \right]^2 \begin{cases} K_n; & \text{for } p = 0, \\ \int z^{2p} k_{nm}(z) dz; & \text{for } p = 1, 2, 3, \dots \end{cases} \quad (60)$$

If we define

$$Q_{nm}^p(z_1) = \int_0^{z_1} z^p k_{nm}(z) dz, \quad (61)$$

and

$$Q_{nm}^0(\infty) = Q_{n0}^0(\infty) = \frac{1}{2} K_n \delta_{m0}, \quad (62)$$

we find that eq. (57) can be written as:

$$\begin{aligned} \mathcal{E} = & -\omega \sum_n e^{in\theta} \sum_{m=0}^{\infty} \frac{n^2}{(N+2m)} \left(\frac{c}{a} \right)^{N+2m} \\ & \times \left\{ K_n \delta_{m0} + \frac{2M}{c} \sum_p \left[b_p Q_{nm}^p(\infty) \delta_{p,\text{even}} + M(M-1) \left(\frac{b_p}{c} \right)^2 Q_{nm}^{2p}(\infty) + \dots \right] \right\}, \end{aligned} \quad (63)$$

where

$$\delta_{p \text{ even}} = \begin{cases} 1 & \text{for } p \text{ even,} \\ 0 & \text{for } p \text{ odd.} \end{cases}$$

We see from eq. (63) that if the coil possesses a linear taper ($p = 1$) then to first order, the taper has no effect if the element is centered about $z = 0$. If the element is not placed at $z = 0$, the first order term integrates to zero, but there will, of course, be an error due to the change, in the effective mean radius c . To second order, there are terms proportional to n^2 for all values of m . This shows that to first order, a rotation of the coil by an angle ϕ about an axis perpendicular to the z -axis will produce no first order error, but will result in even-order harmonics proportional to ϕ^{2l} ; $l = 1, 2, 3, \dots$. Clearly, a quadratic ($p = 2$) error in the coil results in a first order term in (b/c) being present in eq. (63). A term with $p = 0$ is equivalent to a systematic error in the radius of the coil. If the coil "integrates" over only one half of the magnet, the condition $\delta_{p \text{ even}}$ is removed and the first-order term in (b/c) exists for all values of p . An expression similar to eq. (63) holds where the coil integrates over only a small section of the device. In that case, we must replace K_n by the integral $Q_{nm}^0(z_1, z_2)$ and $Q_{nm}^p(\infty)$ by $Q_{nm}^p(z_1, z_2)$ where

$$Q_{nm}^p(z_1, z_2) = \int_{z_1}^{z_2} z^p k_{nm}(z) dz, \quad (64)$$

with $p = 0, 1, 2, \dots$. In general, $|Q_{nm}^p| > 0$ for all m . However, Q_{nm}^p is small for $m > 0$ in the central region of a long device.

4.3. Effects of a torsional error in the coil

Let us suppose that the coil has a torsional error given by $\Delta\theta \propto z^p$. Such errors can arise from misalignment of the coil in the bobbin or from sag and/or associated radial vibrations (see section 4.6). If we set the radial integration limit in eq. (57) equal to c and substitute $\theta + \tau z^p$ for θ in the exponential function, we obtain the following expression after integration over r :

$$\mathcal{E} = -\omega \int_{-\infty}^{\infty} dz \sum_n e^{in\theta} e^{in\tau z^p} \sum_{m=0}^{\infty} \frac{n^2}{(N+2m)} k_{nm}(z) \left(\frac{c}{a}\right)^{N+2m}. \quad (65)$$

The second exponential factor can be expanded in its power series, which leads to the following integral over z :

$$\int_{-\infty}^{\infty} dz k_{nm}(z) \left[1 + in\tau z^p - \frac{(n\tau z^p)^2}{2} - i \frac{(n\tau z^p)^3}{3!} + \dots \right]. \quad (66)$$

The first term is just K_n by virtue of eq. (33); the odd terms are zero by virtue of symmetry. Hence eq. (65) can be written in the form:

$$\mathcal{E} = \omega \sum_n e^{in\theta} \left(\frac{c}{a}\right)^N \left\{ K_n + \sum_{m=0}^{\infty} \frac{n^2 \tau}{(N+2m)} \left(\frac{c}{a}\right)^{2m} [2iQ_{nm}^p(\infty)\delta_{p,\text{even}} - n\tau Q_{nm}^{2p}(\infty) + \dots] \right\}. \quad (67)$$

The last term in square brackets in eq. (67) is finite for all values of m and p by arguments similar to those used to obtain eq. (44). Usually, $N\tau \ll 1$ for all important values of n , so that this term should usually be very small. The first term is non-zero only when p is even if we integrate over all of the magnetic field. Furthermore, we see that even values of p generate both normal and skew ^{#2} spurious components.

4.4. Effects of non-uniform angular velocity and angular vibration

Let us assume a radial coil that includes all of the fringe-field region. The extension to more complicated geometries is straightforward. Let us assume that the nonuniform angular motion can be written as:

$$\theta(t) = \omega_0 t + \omega' t^2 + \sum_{q=-\infty, \neq 0}^{\infty} \theta_q e^{iq\omega_1 t}, \quad (68)$$

where ω_0 is the mean (constant) angular velocity, ω' is its first derivative, and the final term is a Fourier expansion of an angular vibration with coefficients θ_q and fundamental frequency ω_1 . If $\theta(t)$ is to be real then $\theta_{-q}^* = \theta_q$. We assume that changes in the angular velocity of order higher than ω' are negligible, but can be included if necessary. The expansion of the vibration as a Fourier series with some fundamental frequency ω_1 implies a steady-state, periodic situation dominated by a single frequency, but should be a reasonably good approximation if the vibration is the result of a small non-uniformity in the drive mechanism. Vibrations excited by the drive mechanism will usually be periodic. The detailed treatment of the driving terms of such vibrations is outside of the scope of this report, as is the treatment of damping. Nevertheless, the consequences of angular vibrations should be adequately illustrated in this analysis. Substitution of eq. (68) into eqs. (26) and (34) gives

$$\mathcal{E} = - \sum_n N K_n \left(\frac{c}{a}\right)^N e^{in\theta(t)} \left\{ \omega_0 + 2\omega' t + i\omega_1 \sum_q q \theta_q e^{iq\omega_1 t} \right\}. \quad (69)$$

^{#2} The commonly used terms normal and skew refer to the orientation of the multipole. In the normal orientation the principal axis of the multipole is in the x direction, while in the skew orientation, it points in the y or z direction.

We note that the last term, which comes from the angular vibration, could in principle generate an EMF even when the coil is not rotating, if the driving term for the vibration is not associated with the coil drive mechanism. In order to study the consequences of the non-uniform velocity, we expand eq. (69) in a Fourier series with respect to $\theta = \omega t$ as follows:

$$\mathcal{E} = \sum_{m=-\infty}^{\infty} c_m e^{i\lambda_m \theta_0}, \quad (70)$$

where the Fourier coefficients are given by

$$c_m = \frac{1}{2\theta_{\max}} \int_{-\theta_{\max}}^{\theta_{\max}} \mathcal{E} e^{-i\lambda_m \theta_0} d\theta_0; \quad \lambda_m = m\pi/\theta_{\max}. \quad (71)$$

Here we have substituted $t = \theta_0/\omega_0$ in eq. (69) and θ_{\max} is one half of the maximum angular range over which a measurement of the harmonics of the device is to be made; we can assume that $\theta_{\max} = n\pi$ where n is an integer without loss of generality. The number of revolutions n that are incorporated into any given measurement sets the periodicity of the linear frequency error. If this error were due to a bearing catching, for example, then it would have a periodicity of some multiple of 2π and we can set $\theta_{\max} = \pi$. We will make such an assumption now for convenience and treat the case where $n > 1$ later.

If we also assume that both $|n\omega'/\omega_0| \ll 1$ and $|n\sum \theta_q e^{iq\theta_0}| \ll 1$ then the exponential factor containing $\theta(t)$ in eq. (69) can be expanded in a power series with the result that

$$\exp\left\{in\left[\theta_0 + \frac{\omega'}{\omega_0^2}\theta_0^2 + \sum \theta_q e^{iqk\theta_0}\right]\right\} \approx e^{in\theta_0} \left[1 + in\frac{\omega'}{\omega_0^2}\theta_0^2 + \dots\right] \left[1 + in\sum \theta_q e^{iqk\theta_0} + \dots\right], \quad (72)$$

where $k = \omega_1/\omega_0$. Substitution of eq. (72) into eq. (69) leads to

$$c_m = -\sum_n NK_n \left(\frac{c}{a}\right)^N \frac{1}{2\theta_{\max}} \int_{-\theta_{\max}}^{\theta_{\max}} e^{in\theta_0} \left[1 + in\frac{\omega'}{\omega_0^2}\theta_0^2 + \dots\right] \left[1 + in\sum_q \theta_q e^{iqk\theta_0}\right] \\ \times \left\{\omega_0 + 2\frac{\omega'}{\omega_0}\theta_0 + i\omega_1 \sum_q q\theta_q e^{iqk\theta_0}\right\} e^{-i\lambda_m \theta_0} d\theta_0, \quad (73)$$

and we see there are four terms that are first order in the small quantities plus the leading term. If we neglect all terms that are second order or higher, and set $\theta_{\max} = \pi$, we can define the coefficients \mathfrak{A} , \mathfrak{B} , \mathfrak{C} , and \mathfrak{D} by the following integrals (note: $\lambda = m$ if $\theta_{\max} = \pi$):

$$\mathfrak{A}_m^n = \frac{1}{2\pi} \int_{-\pi}^{\pi} e^{i(n-m)\theta_0} d\theta_0 = \frac{\sin[(n-m)\pi]}{(n-m)\pi} = \delta_{nm}, \quad (74)$$

where δ is the Kronecker δ .

$$\mathfrak{B}_{mq}^n = \frac{1}{2\pi} \int_{-\pi}^{\pi} e^{i(n+qk-m)\theta_0} d\theta_0 = \frac{\sin[(n-m+qk)\pi]}{\pi(n-m+qk)} = \frac{(-1)^{n-m} \sin(qk\pi)}{\pi(n-m+qk)}. \quad (75)$$

For $n \neq m$, the coefficient \mathfrak{C}_m^n is

$$\mathfrak{C}_m^n = \frac{1}{2\pi} \int_{-\pi}^{\pi} \theta_0 e^{i(n-m)\theta_0} d\theta_0 = \frac{1}{2\pi} \left\{ \theta_0 \frac{e^{i(n-m)\theta_0}}{i(n-m)} + \frac{e^{i(n-m)\theta_0}}{(n-m)^2} \right\}_{-\pi}^{\pi}, \quad (76)$$

where we have integrated by parts. Eq. (76) reduces to

$$\mathfrak{C}_m^n = -i \frac{\cos[(n-m)\pi]}{n-m} + i \frac{\sin[(n-m)\pi]}{\pi(n-m)^2}. \quad (77)$$

We see that the second term on the right-hand side of eq. (77) is zero. Eq. (77) is clearly divergent when $n = m$. Nevertheless, direct integration of the left-hand side of eq. (76) for $n = m$ indeed gives zero as the function is odd. Thus we obtain the result

$$\mathfrak{E}_m^n = \begin{cases} 0; & \text{if } n = m, \\ -i \frac{(-1)^{n-m}}{n-m}; & \text{if } n \neq m. \end{cases} \quad (78)$$

In a similar fashion, we find that

$$\mathfrak{D}_m^n = \frac{1}{2\pi} \int_{-\pi}^{\pi} \theta_0^2 e^{i(n-m)\theta_0} d\theta_0 = \frac{1}{2\pi} \left\{ \theta_0^2 \frac{e^{i(n-m)\theta_0}}{i(n-m)} - 2 \int \theta_0 \frac{e^{i(n-m)\theta_0}}{i(n-m)} d\theta_0 \right\}_{-\pi}^{\pi}. \quad (79)$$

The second term on the right hand side of eq. (79) is just $2\mathfrak{E}/[i(n-m)]$, and the first term is zero if $n \neq m$. If $n = m$ the integral of the right hand side of eq. (79) is $\pi^2/3$. This can be summarized as follows:

$$\mathfrak{D}_m^n = \begin{cases} \pi^2/3; & n = m, \\ 2 \frac{(-1)^{n-m}}{(n-m)^2}; & n \neq m. \end{cases} \quad (80)$$

With the approximations as described, we see that the coefficients \mathfrak{B} , \mathfrak{E} , and \mathfrak{D} appear as “dispersion functions” that mix the angular vibrations with the true harmonics, producing “side-bands” of spurious “harmonics” that do not in fact exist in the magnetic field. Finally, we can write the new Fourier expansion for the EMF as

$$\mathcal{E} = - \sum_{m=-\infty}^{\infty} NK_n \left(\frac{c}{a} \right)^n e^{im\theta_0} \left\{ \omega_0 \delta_{nm} + i \sum_q (n + \omega_1 q) \theta_q \mathfrak{B}_{mq}^n + 2 \frac{\omega'}{\omega_0} \mathfrak{E}_m^n + in \frac{\omega'}{\omega_0^2} \mathfrak{D}_m^n \right\}. \quad (81)$$

We see from eqs. (74)–(80) and (81) that both the angular vibration terms and the linear angular velocity terms are purely imaginary (note that \mathfrak{E} is intrinsically imaginary) and appear as spurious “skew” components in the field. Unlike the situation represented by eqs. (26) and (44), where we had components with n -pole symmetry, but with the radial dependence of a higher multipole, here we have components with higher multipolarity, but with the radial dependence of its “fundamental”. We also observe that all of the spurious components are strongly peaked and centered on or near each of the real harmonics present in the magnetic field (for the case where ω_1/ω_0 is not a rational fraction). Thus the non-uniform angular motion spreads the real harmonics into adjacent harmonics with, except for the last term in eq. (81), a $1/(n-m)$ dependence. Therefore, one wants to design a system that minimizes the vibrations. Furthermore, the rotational frequency ω_0 should be chosen so that the separation between natural vibrational frequencies and $n\omega_0$ is as large as possible for all harmonics, n , of importance. We should also note that the absolute value of the strength of the fundamental component is modified by the terms \mathfrak{B} and \mathfrak{D} in eq. (81), even if we are not concerned about spurious harmonics. Those spurious harmonics that lie on top of real components will not only change the measured amplitude of the harmonic, but also change its apparent phase since the spurious components are skew. If ω_1 is an integer multiple of ω_0 then k is an integer and we see from eq. (75) that $\mathfrak{B} = 0$ unless $n - m + qk = 0$. Hence the vibrational term in eq. (81) generates a single discrete spurious harmonic for each allowed value of n and q .

Because the spreading strength is assumed to be small, the biggest problem with harmonic contamination occurs for the fundamental harmonic which can be 1000 times stronger than the other harmonics present in the magnetic field. In such cases, bucking coils provide an obvious solution. We see immediately by substituting eq. (81) into eq. (49) that if the vibrational modes are common to both coils

then the spurious harmonics generated by the fundamental harmonic will be canceled. The use of bucking coils is essential if accurate measurements of the “harmonic content” of a device is required. Even with bucking coils one can have problems if the mapping machine has not been carefully designed and constructed, because the n and q -dependence of the vibrational amplitude enhances the effects for the higher harmonics; this could be a severe problem if a vibrational mode were resonant.

Finally, we consider the case where a measurement is made over many rotational periods such that $\theta_{\max} = n\pi$ in eq. (73). We see that all of the above results are valid if we replace n in (81) by $n\pi$. The apparent frequency of the magnetic harmonics now appear to be π time higher, but this is exactly the result we would obtain if we analyzed such a spectrum with an FFT routine, for example. We should also point out here that the Fourier expansion of the uniform velocity “ramp” is only conditionally convergent at the end points. That should not affect the results presented here.

4.5. Effects of non-uniform bin width in the integration of the EMF

In section 3.1 we saw that the result of the integration of the EMF was independent of the rotational frequency. We are, however, trading one set of problems for another because now we must rely on the uniformity of the angular encoder that determines the bin width $2\delta\theta$. One advantage of integration, though, is that once the non-uniformities in the angular encoder are known they should be reproducible. That will not usually be the case for a non-integrating system. As in section 4.4, let us expand the non-uniformity in the angle encoder in a Fourier series as follows:

$$\theta = \theta_0 + \sum_{s=-N/2+1}^{N/2-1} \mathcal{A}_s e^{is\theta_0}, \quad (82)$$

where N is the number of bins. As before, if θ is to be real, $\mathcal{A}_{-s}^* = \mathcal{A}_s$. The bin width at any given angle j is just

$$2\delta\theta_j = [\theta_{j+1} - \theta_j] = 2\delta\theta_{0j} + \sum_s \mathcal{A}_s e^{is(\theta_{0j} + \delta\theta_{0j})} - \sum_s \mathcal{A}_s e^{is(\theta_{0j} - \delta\theta_{0j})} \quad (83)$$

where θ_{0j} is the center of the unperturbed bin between θ_{j+1} and θ_j . On expansion of the Fourier series in eq. (83), we find that $\delta\theta_j$ is

$$\delta\theta_j = \delta\theta_{0j} + i \sum_s \mathcal{A}_s e^{is\theta_{0j}} \sin(s\delta\theta_{0j}). \quad (84)$$

If we substitute eq. (84) into eq. (47) we obtain the result:

$$Q = i \sum_n K_n \left(\frac{c}{a} \right)^N \{ e^{in(\theta_0 + \delta\theta)} - e^{in(\theta_0 - \delta\theta)} \}, \quad (85)$$

where we have dropped the subscript j for convenience. If we assume that the angular non-uniformity is small and expand the exponential term for the non-uniformity as we did in eq. (72), we obtain

$$\begin{aligned} Q &= i \sum_n K_n \left(\frac{c}{a} \right)^N e^{in\theta_0} \left\{ e^{in\delta\theta_0} \left[1 - n \sum_{s=-\infty}^{\infty} \mathcal{A}_s e^{is\theta_0} \right] - e^{-in\delta\theta_0} \left[1 + n \sum_{s=-\infty}^{\infty} \mathcal{A}_s e^{is\theta_0} \right] \right\} \\ &= -2 \sum_n K_n \left(\frac{c}{a} \right)^N e^{in\theta_0} \left\{ \sin(n\delta\theta_0) + in \cos(n\delta\theta_0) \sum_{s=-\infty}^{\infty} \mathcal{A}_s e^{is\theta_0} \right\} \end{aligned} \quad (86)$$

Finally, we substitute eq. (82) for θ in eq. (86) and expand the perturbation term as before

$$Q = -2 \sum_n K_n \left(\frac{c}{a} \right)^N e^{in\theta_0} \left[1 + in \sum_{s=-\infty}^{\infty} \mathcal{A}_s e^{is\theta_0} \right] \left\{ \sin(n\delta\theta_0) + in \cos(n\delta\theta_0) \sum_{s=-\infty}^{\infty} \mathcal{A}_s e^{is\theta_0} \right\}. \quad (87)$$

If we now expand eq. (87) in a new Fourier series, as we did in the previous section (see eqs. (70) and (71) and drop all terms that are second order in ω' , we find that

$$Q = -2 \sum_{n=-\infty}^{\infty} K_n \left(\frac{c}{a} \right)^N e^{im\theta_0} \left\{ \sin(n\delta\theta_0) \delta_{n,m} + in [\sin(n\delta\theta_0) + \cos(n\delta\theta_0)] \sum_{s=-\infty}^{\infty} \psi_s \delta_{n+s,m} \right\}. \quad (88)$$

Once again we see that spurious harmonics are generated by the non-uniformities in the angular encoder. If the errors in bin width are random, we see that the spurious harmonics will be of very high frequency, but if there are correlated errors with low frequency, they will not only generate “side bands” but will also modify the amplitude of the real harmonics being measured.

4.6. Effect of radial vibrations and sag of the coil

We assume once again a radial coil that includes “all” of the fringe-field region. The extension to more complicated geometries can be made in a straightforward manner. The treatment of radial vibrations is more difficult than that for angular vibrations, because the modes of vibration of a stiff bar or cylinder [13] are not necessarily “harmonic”. Furthermore, the shape of the radial distortion as a function of z is also not necessarily “harmonic”, so neither the frequency nor the distortion modes of the coil can, in general, be represented by single terms of a Fourier series. As a consequence, we will deal explicitly with the lowest three modes. The extension to higher modes, which in general should not be necessary, is obvious.

As in the previous discussion of angular vibrations, we will not attempt to deal in detail with the driving term (except for coil sag), because this is intimately connected with the details of the machine and its environment. Neither will we discuss damping of the vibrations, as our aim is to show the consequences in principle of such vibrations on the measured spectrum, not to be a treatise on the subject of mechanical vibration.

The equation of motion for a stiff object is [13]

$$\frac{\partial^4 r}{\partial z^4} + \frac{\rho}{E\kappa^2} \frac{\partial^2 r}{\partial t^2} = 0, \quad (89)$$

where ρ is the density of the coil bobbin, E is Young’s Modulus and κ is the radius of gyration defined by the integral

$$\kappa = \frac{1}{A} \int r^2 dA, \quad (90)$$

where A is the area of the cross section of the bobbin. The solution of eq. (89) can be written in the form [13].

$$r = Y(z) e^{+i\omega_n t}, \quad (91)$$

where ω_n is one of the allowed normal modes of vibration and $Y(z)$ is given by

$$Y(z) = C_1 e^{\mu_n z} + C_2 e^{-\mu_n z} + C_3 e^{i\mu_n z} + C_4 e^{-i\mu_n z}. \quad (92)$$

The angular frequency ω_n and scaling parameter μ_n are related by the expression:

$$\omega_n = \kappa \mu_n^2 \sqrt{E/\rho}. \quad (93)$$

We will consider two classes of particular solutions to eq. (93) that depend upon the specific boundary conditions we assume at the ends of the bobbin (as in all the previous discussion we set the origin of the z axis in the center of the coil bobbin). They are:

1. Both ends are fixed in position but allowed to rotate about the fixed points. Hence

$$\begin{aligned} Y(-L/2) &= Y(L/2) = 0, \\ \frac{d^2 Y}{dz^2} &= 0 \quad \text{at} \quad z = \pm L/2, \end{aligned} \quad (94)$$

2. Both ends are rigidly clamped. Hence

$$\begin{aligned} Y(-L/2) &= Y(L/2) = 0, \\ \frac{dY}{dz} &= 0 \quad \text{at} \quad z = \pm L/2, \end{aligned} \quad (95)$$

where L is the length of the bobbin. As we shall see, class 1 leads to “harmonic” motion while class 2 does not.

From the assumed symmetry and from the boundary conditions eq. (94) for class 1, we see that both C_1 and C_2 in eq. (92) must be zero. Furthermore, $|C_3| = |C_4|$, which leads to

$$\begin{aligned} Y(z) &= A \cos(\mu z) \quad \text{Even,} \\ Y(z) &= B \sin(\mu z) \quad \text{Odd,} \end{aligned} \quad (96)$$

where A and B are constants derivable from $C_3 - C_4$. The allowed values of μ are determined from the boundary condition that

$$\begin{aligned} Y = d^2 Y / dz^2 &= \cos(\mu L/2) = 0, \\ \text{or } Y = d^2 Y / dz^2 &= \sin(\mu L/2) = 0, \end{aligned} \quad (97)$$

respectively. Thus the two cases form a Fourier series and, in this case, the solutions are harmonic with angular frequencies given by eq. (93). The lowest frequency clearly occurs when $\mu = \pi/L$.

In general, the radial vibrations will occur at some angle ϑ with respect to the plane passing through the coil. Hence, the vibration will produce effects which have components that are a combination of an oscillating radial and tangential error in the coil. If we define the x -axis of the coil to lie in the plane of a radial coil or to be the bisector of a tangential coil, then the radial component is given by

$$r = r \cos(\vartheta), \quad (98)$$

and the tangential component by

$$t = r \sin(\vartheta) \quad (99)$$

where r is given by eq. (91).

4.6.1. Bobbin ends allowed to rotate about the fixed points

Let us treat first the situation where the coil vibrates in its fundamental mode with small amplitude and the coil-bearing system satisfies the boundary conditions for class 1, so that the radial shape of the coil is given by

$$F(z, t) = c + \cos(\mu_1 z) [b e^{i\omega_1 t} + b^* e^{-i\omega_1 t}] \Rightarrow c + \cos(\mu_1 z) b^+ e^{\pm i\omega_1 t}, \quad (100)$$

where $b = C_3 \cos(\vartheta) = A/2 e^{i\varphi} \cos(\vartheta)$, $b^* = C_4 \cos(\vartheta) = A/2 e^{-i\varphi} \cos(\vartheta)$ represent the amplitude of the vibration and we have substituted the lowest order solution of eq. (96) into eq. (91); φ is the phase of the vibration. The \pm notation means that we sum the two solutions as indicated in [...]; b^+ is to be interpreted as b and b^- as b^* . The induced voltage in a rectangular coil that includes “all” of the flux is

found by substituting eq. (100) into eq. (34) with B_θ given by eq. (26). As in section 4.2, we perform the integration over r to obtain the result

$$\mathcal{E} = i \frac{d}{dt} \int_{-L/2}^{L/2} dz \sum_n e^{in\theta} \sum_{m=0}^{\infty} \frac{n}{M} k_{nm}(z) \left[\frac{c + b^+ \cos(\mu_1 z) e^{\pm i\omega_1 t}}{a} \right]^M. \tag{101}$$

Since we have assumed that $|b| \ll c$, we can expand the square-bracketed factor in a binomial series as was done in eq. (58) and perform the integration over z :

$$\int_{-L/2}^{L/2} [\dots]^{N+2m} dz = \int \left(\frac{c}{a} \right)^M \left\{ 1 + M \left[\frac{b^+ \cos(\mu_1 z) e^{\pm i\omega_1 t}}{c} \right] + \dots \right\} k_{nm}(z) dz, \tag{102}$$

where $M = |n| + 2m$. The first term in eq. (102) is just K_n if the coil is long enough to include “all” of the flux. The second term can be written in the form

$$\int_I dz = \frac{b^\pm M}{2c} e^{\pm i\omega_1 t} \int_{-L/2}^{L/2} [e^{i\mu_1 z} + e^{-i\mu_1 z}] k_{nm}(z) dz, \tag{103}$$

where we have substituted the exponential form for $\cos(\mu_1 z)$. Now we substitute eq. (22) for k_{nm} and interchange the order of integration with respect to ν and z . Hence

$$\int_I dz = \frac{b^\pm M}{2c} e^{\pm i\omega_1 t} \ell_{nm} \int_{-\infty}^{\infty} W_{nm}(\nu) d\nu \int_{-L/2}^{L/2} [e^{i\mu_1 z} + e^{-i\mu_1 z}] e^{i\nu z} dz, \tag{104}$$

where

$$\ell_{nm} = \frac{a^{2m}}{m!(N+m)!}.$$

Since we have assumed that the coil is long enough to include “all” of the fringe field, we can replace $\pm L/2$ by $\pm \infty$ with negligible error. From eq. (31) we see that the integration over z in eq. (104) is just

$$\int_{-\infty}^{\infty} \dots dz = 2\pi [\delta(\nu + \mu_1) + \delta(\nu - \mu_1)],$$

and thus eq. (104) becomes

$$\int_I dz = \frac{b^\pm M}{2c} e^{\pm i\omega_1 t} \ell_{nm} \int_{-\infty}^{\infty} W_{nm}(\nu) 2\pi [\delta(\nu + \mu_1) + \delta(\nu - \mu_1)] d\nu. \tag{105}$$

If the lens is symmetric about $z = 0$, then $W_{nm}(\nu)$ is an even function of ν and eq. (105) reduces to

$$\int_I dz = \frac{2\pi M b^\pm}{c} e^{\pm i\omega_1 t} \ell_{nm} W_{nm}(\mu_1) \delta(\nu - \mu_1). \tag{106}$$

Hence eq. (101) can be written in the form

$$\mathcal{E} = i \frac{d}{dt} \sum_n e^{in\theta} \sum_{m=0}^{\infty} \frac{n}{M} \left(\frac{c}{a} \right)^M \left\{ K_n \delta_{m0} + \frac{2\pi M b^\pm}{c} K_{nm}(\mu_1) e^{\pm i\omega_1 t} + \dots \right\}, \tag{107}$$

where

$$K_{nm}(\mu) = \ell_{nm} W_{nm}(\mu). \tag{108}$$

Even if we integrate eq. (107) as in section 3.1, the spurious terms do not disappear. Hence integration does not eliminate the effects of radial vibrations, but it does reduce the amplitude by a factor of $n/(n \pm k)$ (see eq. (109)). If we assume a constant angular frequency ω so that $\theta = \omega t$ and define $\theta_1 = \omega_1 t$, then we find on differentiation with respect to t that

$$\mathcal{E} = -\omega \sum_n e^{in\theta} \sum_{m=0}^{\infty} \frac{n}{M} \left(\frac{c}{a}\right)^M \left\{ nK_n \delta_{m0} + \frac{2\pi M b^+}{c} (n \pm k) K_{nm}(\mu_1) e^{\pm i\theta_1} \right\}, \quad (109)$$

where $k = \omega_1/\omega$ and the $\pm k$ means both signs of k are included in the sum with b^+ . We see that, in principle, all values of m are allowed for the second term in eq. (109). As in section 4.4, we expand eq. (109) in a new Fourier series expressed entirely in terms of $\theta = \omega t$ according to eqs. (70) and (71). The first term in eq. (109) is just δ_{nm} by virtue of eq. (74) and the second term is just \mathfrak{B}_{m1}^n where we set $r = 1$. The final result is:

$$\mathcal{E} = -\omega \sum_{n=-\infty}^{\infty} e^{in\theta} \sum_{m=0}^{\infty} \frac{n}{M} \left(\frac{c}{a}\right)^M \left\{ nK_n \delta_{m0} \delta_{nm} + \frac{2\pi M b^+}{c} (n \pm k) K_{nm}(\mu_1) \frac{(-1)^{n-m} \sin(\pm k\pi)}{(n-m \pm k)\pi} \right\}. \quad (110)$$

From eq. (110) we see that, as for angular vibrations (section 4.4), the radial component of the vibration introduces sets of spurious side bands centered in the vicinity of each of the real harmonics n in the magnetic field. In addition, we see that the vibration also introduces effects from the fringing field regions of the lens via the ‘‘Bessel’’ terms, as in section 4.2.

Now we treat the tangential component of the vibration considered above. The treatment will be similar to the treatment of the torsional error (section 4.3). By definition, eq. (99), the tangential component of the radial vibration only produces a z -dependent variation in the azimuthal angle θ , which is given by

$$\theta(t, z) = \omega t + \frac{1}{c} \cos(\mu_1 z) [\tau^+ e^{i\omega_1 t} + \tau^- e^{-i\omega_1 t}] \Rightarrow \omega t + \frac{1}{c} \cos(\mu_1 z) \tau^\pm e^{\pm i\omega_1 t}, \quad (111)$$

where $\tau^+ = C_3 \sin(\vartheta) = A/2 e^{i\varphi} \sin(\vartheta)$ and $\tau^- = C_4 \sin(\vartheta) = A/2 e^{-i\varphi} \sin(\vartheta)$, where φ is the phase angle of the vibration; as before, the \pm notation means that we sum over both solutions. We substitute eq. (26) into eq. (34) and integrate with respect to r to obtain

$$\mathcal{E} = i \frac{d}{dt} \int_{-L/2}^{L/2} dz \sum_n e^{in\theta(t,z)} \sum_{m=0}^{\infty} \frac{n}{M} k_{nm}(z) \left(\frac{c}{a}\right)^M. \quad (112)$$

If we expand the exponential factor involving $\theta(t, z)$ in eq. (112) in an identical manner to eq. (67) and retain only the first two terms, we obtain

$$\mathcal{E} = i \frac{d}{dt} \int_{-L/2}^{L/2} dz \sum_n e^{in\omega t} \left[1 + \frac{in\tau^\pm}{c} \cos(\mu_1 z) e^{\pm i\omega_1 t} \right] \sum_{m=0}^{\infty} \frac{n}{M} k_{nm}(z) \left(\frac{c}{a}\right)^M. \quad (113)$$

We see that the second term in [...] in eq. (113) is similar in form to eq. (102) and can be treated in an identical manner. The result of the integration with respect to z can be obtained by inspection and is

$$\mathcal{E} = i \frac{d}{dt} \sum_n e^{in\omega t} \sum_{m=0}^{\infty} \frac{n}{M} \left(\frac{c}{a}\right)^M \left\{ K_n \delta_{m0} + \frac{2\pi in\tau^\pm}{c} K_{nm}(\mu_1) e^{\pm i\omega_1 t} + \dots \right\}. \quad (114)$$

Note also, that integration of eq. (114) with respect to t does not eliminate the spurious terms. Hence integration does not eliminate the effects of either the radial or the tangential components of the radial

vibrations, but it does reduce the amplitude by a factor of $n/(n \pm k)$ (see eq. (109)). On differentiating eq. (114) with respect to t we obtain

$$\mathcal{E} = -\omega \sum_n e^{in\theta} \sum_{m=0}^{\infty} \frac{n}{M} \left(\frac{c}{a}\right)^M \left\{ nK_n \delta_{m0} + \frac{2\pi i n \tau^+}{c} (n \pm k) K_{nm}(\mu_1) e^{+i\theta_1} \right\} \quad (115)$$

where as earlier $\pm k$ means that the appropriate sign of k is used in the sum τ^+ . If we expand eq. (115) in a new Fourier series as we did with eq. (109), we obtain once more by inspection that

$$\mathcal{E} = -\omega \sum_{m=-\infty}^{\infty} e^{im\theta} \sum_{n=0}^{\infty} \frac{n}{M} \left(\frac{c}{a}\right)^M \left\{ nK_n \delta_{m0} \delta_{nm} + \frac{2\pi i n \tau^+}{c} (n \pm k) K_{nm}(\mu_1) \frac{(-1)^{n-m} \sin(\pm k\pi)}{(n-m \pm k)\pi} \right\}. \quad (116)$$

We see from an inspection of eqs. (116) and (110) that the radial and tangential components of the vibration produce similar results but with two significant differences. The first is that the vibration generates imaginary or skew terms for the spurious harmonics in the tangential direction, and secondly the strength of the spurious radial terms are proportional to M instead of n as in the tangential case. From eqs. (105) and (106), we see that the odd class of solutions given in eq. (96) do not generate spurious harmonics to first order in the expansion so only even-class solutions need be studied. The treatment of other even class vibrations is identical to the treatment given above.

We will now investigate the effects of the coil sagging under its own weight. The differential equation for the deflection of a uniformly loaded beam is [14]

$$EI \frac{d^4 r}{dz^4} = w, \quad (117)$$

where $I = \kappa^2 A$ is the “moment of inertia of the cross section”, and w is the force per unit length. This equation is similar to the time independent part of eq. (89) and has solutions of the form:

$$r(z) = \sum_{p=0}^4 C_p z^p. \quad (118)$$

We see directly from substituting eq. (118) into the differential equation that

$$C_4 = \frac{w}{24EI} \quad (119)$$

From the assumed symmetry, we find that $C_3 = C_1 = 0$ (equivalent to the lowest mode of vibration). The boundary conditions for class 1, eq. (94) imply that

$$C_0 = \frac{5}{16} L^4 C_4, \quad (120)$$

and

$$C_2 = -\frac{3}{2} L^2 C_4. \quad (121)$$

Hence eq. (118) can be written as

$$r(z) = C_4 L^4 \left\{ \frac{5}{16} - \frac{3}{2} \left(\frac{z}{L}\right)^2 + \left(\frac{z}{L}\right)^4 \right\}. \quad (122)$$

We see that eq. (122) has the same form as eq. (56). Hence we can carry over all of the analysis of section 4.2 and 4.3 on a z -dependent deformation of the coil to the case of the coil sagging under its own

weight. It is also clear that as the coil rotates both radial and tangential "vibrations" will be excited at the rotational frequency, ω (see eqs. (98) and (99)) and that the first term in eq. (122) produces a sinusoidally varying error in the mean radius, c , of the coil.

In the previous discussion of vibrations, we have ignored the driving terms, and have implicitly assumed that there is weakly coupled non-resonant excitation of the natural vibrational modes of the coil with low amplitude. In the case of coil sag, we have a strongly coupled driving term, which is presumably not resonant with the natural modes of vibration, that determines the frequency of vibration. (Usually the natural radial modes will have frequencies in the hundreds of Hz to kHz domain which is widely separated from the rotational frequency of ≈ 1 Hz.) Hence it is reasonable to assume that the driving term (the rotation of the coil bobbin) allows adiabatic relaxation of the coil shape into the form given by eq. (122). Another important difference is that the driving term and hence the oscillation does not have a constant phase angle ϑ with respect to the coil, but precesses with exactly the angular frequency of the coil. Consequently, both the radial and tangential components are always excited to full amplitude. Finally, we see from fig. 1 that the driving term is phase shifted by $-\pi/2$ with respect to the coordinate system assumed in this analysis. Taking into account the points discussed above, we obtain

$$F(z, t) = c - \sin(\omega t + \varphi) \sum_{p=0}^4 C_p z^p \Rightarrow c + \frac{i}{2} e^{\mp i\varphi} e^{\pm i\omega t} \sum_{p=0}^4 C_p z^p, \quad (123)$$

and

$$\theta(z, t) = \omega t + \cos(\omega t + \varphi) \sum_{p=0}^4 C_p z^p \Rightarrow \omega t + \frac{1}{2} e^{\pm i\varphi} e^{\pm i\omega t} \sum_{p=0}^4 C_p z^p, \quad (124)$$

where the \pm denotes the sum of the angular solution plus its complex conjugate as before and φ is a phase which accounts for an angular misalignment of the apparatus. If we substitute eq. (123) into eq. (57) or equivalently eq. (101), and make use of the results of section 4.2 and the procedures leading to eq. (110), we find by inspection that the radial component is

$$\begin{aligned} \mathcal{E} = & -\omega \sum_{m=-\infty}^{\infty} e^{im\theta} \sum_{n=0}^{\infty} \frac{n}{M} \left(\frac{c}{a} \right)^M \\ & \times \left\{ nK_n \delta_{nm} \delta_{m0} + M i e^{\pm i\varphi} \sum_{p=0}^4 \frac{C_p}{c} (n \pm 1) Q_{nm}^p(\infty) \frac{(-1)^{n-m} \sin(\pm \pi)}{(n-m \pm 1)\pi} \right\}, \end{aligned} \quad (125)$$

which reduces to

$$\mathcal{E} = -\omega \sum_{m=-\infty}^{\infty} e^{im\theta} \sum_{n=0}^{\infty} \frac{n}{M} \left(\frac{c}{a} \right)^M \left\{ nK_n \delta_{nm} \delta_{m0} + M i e^{\pm i\varphi} \sum_{p=0}^4 \frac{C_p}{c} (n \pm 1) Q_{nm}^p(\infty) \delta_{m, n \pm 1} \right\}. \quad (126)$$

Similarly, if we substitute eq. (124) into eq. (65) or eq. (112) and make use of the results of section 4.3 and the procedures leading to eq. (116), we obtain the tangential component

$$\mathcal{E} = -\omega \sum_{m=-\infty}^{\infty} e^{im\theta} \sum_{n=0}^{\infty} \frac{n}{M} \left(\frac{c}{a} \right)^M \left\{ nK_n \delta_{m0} \delta_{nm} + n i e^{\pm i\varphi} \sum_{p=0}^4 \frac{C_p}{c} (n \pm 1) Q_{nm}^p(\infty) \delta_{m, n \pm 1} \right\}. \quad (127)$$

Even though eq. (96) is not a solution of eq. (117), it is very nearly a solution, as can be seen from fig. 4, and it is perhaps instructive to substitute eq. (96) for eq. (122) in eqs. (123), (124), (126) and (127). In particular, the boundary conditions lead to the same value for μ for the lowest mode of "vibration".

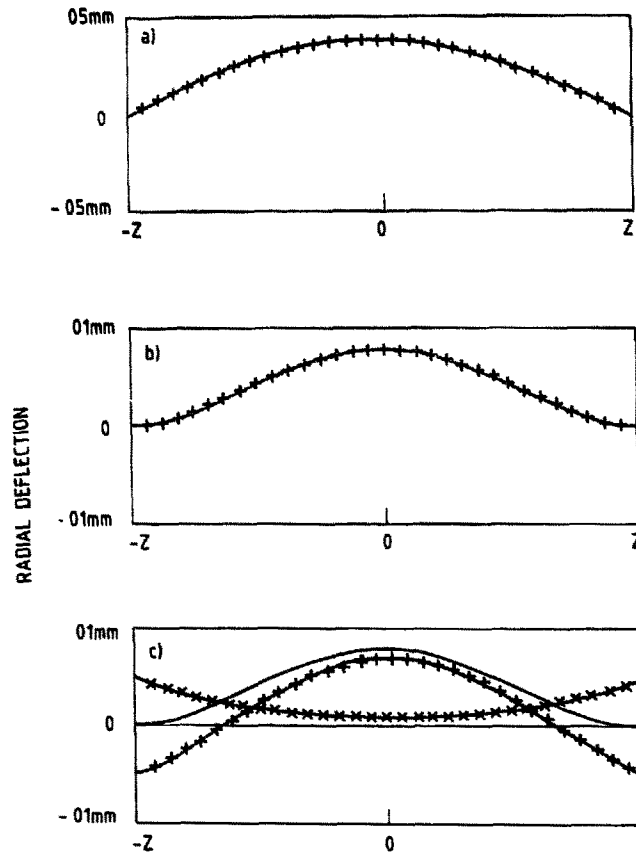


Fig. 4. (a) Comparison of the solution of eq (89) for radial vibrations (+) with that of eq (117) for the coil sagging under its own weights (solid line) for the Class 1 boundary conditions (bobbin ends allowed to rotate about the ends) section 4.6.1. (b) Same as (a) except for Class 2 boundary conditions (bobbin ends rigidly clamped) section 4.6.2. (c) Decomposition of the solution of (89) (solid) into the $\cos(\mu z)$, (+), and $\cosh(\mu z)$ (x) components.

namely μ_1 (see eq. (93)). However, the vibrational frequency, ω , is now not related to μ . On setting $\omega_1 = \omega$ ($k = 1$) and noting that $|b| = |\tau| = A$, eqs. (110) and (116) reduce to

$$\mathcal{E} = -\omega \sum_{n=-\infty}^{\infty} e^{im\theta} \sum_{m=0}^{\infty} \frac{n}{M} \left(\frac{c}{a} \right)^M \left\{ nK_n \delta_{m0} \delta_{nm} + i \frac{\pi MA}{c} (n \pm 1) K_{nm}(\mu_1) \delta_{m,n \pm 1} \right\}, \quad (128)$$

$$\mathcal{E} = -\omega \sum_{n=-\infty}^{\infty} e^{im\theta} \sum_{m=0}^{\infty} \frac{n}{M} \left(\frac{c}{a} \right)^M \left\{ nK_n \delta_{m0} \delta_{nm} + i \frac{\pi nA}{c} (n \pm 1) K_{nm}(\mu_1) \delta_{m,n \pm 1} \right\}, \quad (129)$$

for the radial and tangential components respectively, which not surprisingly, have exactly the same form as eqs. (126) and (127). (Note the the second term in each of eqs. (126) and (128) has been multiplied by $-i$ to account for the phase shift in the driving term.) We see that coil sag generates spurious harmonics with multipolarities $n \pm 1$ for each of the magnetic harmonics that exist in the lens element. For example, the coil sag will produce a “strong” spurious sextupole component (as well as a dipole component) in the spectrum of a quadrupole lens. In view of the fact that the true sextupole should be zero in a perfect quadrupole, and will be very small in any well-made element, this spurious component could easily dominate the true component by a large factor.

Finally, since in any well-designed system, the natural vibrational modes will have frequencies well above that of the highest harmonic of interest, coil sag should be the only major problem. It is clearly advantageous to design the coil bobbin out of materials that are as stiff as possible and to arrange its geometry so that it is as light as possible in order to ensure the above.

As we saw in section 4.4 for the case of angular vibrations, bucking coils are also very useful in reducing the contamination of the higher magnetic harmonics by spurious harmonics coming from coupling of the radial vibrations to the strong fundamental harmonic in the magnetic field. As long as the bucking coils are rigidly connected to the main coils, so their curvature is concentric with the curvature from the sag of the coil bobbin, the bucking coils should also remove most of the spurious $n \pm 1$ components that arises from sagging of the coil.

4.6.2. Coil bobbin ends are rigidly clamped

Now let us consider the situation where the coil vibrates in its fundamental mode with small amplitude and where the coil bearing system satisfies the boundary conditions for case 2; i.e. they are rigidly clamped. From eqs. (91) and (92), and the symmetry assumed for the problem, we see that

$$Y(z) = A[\cos(\mu z) + \ell \cosh(\mu z)]. \quad (130)$$

The value of μ is found from substituting eq. (130) into eq. (95) which after eliminating ℓ leads to the following equation for μ :

$$\cos(\mu L/2) \sinh(\mu L/2) + \sin(\mu L/2) \cosh(\mu L/2) = 0, \quad (131)$$

with

$$\ell = -\frac{\cos(\mu L/2)}{\cosh(\mu L/2)}. \quad (132)$$

The angular frequency of the vibration is given by eq. (93), but now the different modes of vibration are not harmonically related and do not form a Fourier series. We will restrict our discussion here to the lowest mode. Higher modes can be computed in an analogous manner to that given in the previous section. The radial shape of the coil is given by

$$F(z, t) = c + b^\pm [\cos(\mu_1 z) + \ell \cosh(\mu_1 z)] e^{\pm i\omega_1 t} \quad (133)$$

where $b^+ = C_3 \cos(\vartheta) = A/2 e^{i\varphi} \cos(\vartheta)$, $b^- = C_4 \cos(\vartheta) = A/2 e^{-i\varphi} \cos(\vartheta)$ and we use the \pm convention as before. Once again, φ is the phase of the vibration. Under identical conditions to those for eq. (101), we obtain, for the induced EMF in the coil, the result

$$\mathcal{E} = i \frac{d}{dt} \int_{-L/2}^{L/2} dz \sum_n e^{in\theta} \sum_{m=0}^{\infty} \frac{n}{M} k_{nm}(z) \left[\frac{c + b^\pm Y(z) e^{\pm i\omega_1 t}}{a} \right]^M, \quad (134)$$

where $Y(z)$ is given by eq. (130). Since we have assumed that $|b| \ll c$, we can expand the square bracketed factor in a binomial series, as was done in eq. (102), and perform the integration over z :

$$\int_{-L/2}^{L/2} [\dots]^{N+2m} dz = \int \left(\frac{c}{a} \right)^M \left\{ 1 + M \left[\frac{b^\pm Y(z) e^{\pm i\omega_1 t}}{c} \right] + \dots \right\} k_{nm}(z) dz, \quad (135)$$

where $M = N + 2m$. The first term in eq. (135) is just K_n if the coil is long enough to include "all" of flux. The second term can be broken into two integrals over z , involving the \cos and \cosh terms in eq. (130). The $\cos(\mu z)$ integral is identical to that given by eq. (106) except that now, of course, μ_1 is given by eq. (131). In an analogous manner to eqs. (103) and (104), the $\cosh(\mu z)$ term can be written in the form

$$\int_I dz = \frac{b^\pm \ell M}{2c} e^{\pm i\omega_1 t} k_{nm} \int_{-\infty}^{\infty} W_{nm}(\nu) d\nu \int_{-L/2}^{L/2} [e^{\mu_1 z} + c^{-\mu_1 z}] e^{i\nu z} dz, \quad (136)$$

where

$$k_{nm} = \frac{a^{2m}}{m!(|n|+m)!}.$$

The integral over z can be written as

$$\int_H dz = \int_{-L/2}^{L/2} e^{(\pm\mu + i\nu)z} dz = \frac{1}{(\pm\mu + i\nu)} e^{(\pm\mu + i\nu)z} \Big|_{-L/2}^{L/2}, \quad (137)$$

which when expanded and rearranged leads to

$$\int_H dz = \frac{4}{\mu^2 + \nu^2} \left\{ i\mu \sinh\left(\mu \frac{L}{2}\right) \cos\left(\nu \frac{L}{2}\right) + \nu \cosh\left(\mu \frac{L}{2}\right) \sin\left(\nu \frac{L}{2}\right) \right\}. \quad (138)$$

Here we have dropped the subscript on μ for convenience. On substitution of eq. (138) into eq. (136), we are left with the following integral over ν

$$\int_I dz = \frac{2b^{\pm} \ell M}{c} e^{\pm i\omega_1 t} k_{nm} \int_0^{\infty} \frac{W_{nm}(\nu)}{\mu^2 + \nu^2} \left\{ i\mu \sinh\left(\mu \frac{L}{2}\right) \cos\left(\nu \frac{L}{2}\right) + \nu \cosh\left(\mu \frac{L}{2}\right) \sin\left(\nu \frac{L}{2}\right) \right\} d\nu. \quad (139)$$

The integral over ν now ranges from 0 to ∞ because of the use of the standard trigonometric functions instead of the exponential form. We see that the denominator in the integral acts as a strong filter, rapidly suppressing the high “frequency” components in the Fourier transform of the z -dependent part of the potential, especially in the first term; see eqs. (18), (19), and (139). This filtering action will effectively broaden the fringe-field region and thus one must be certain that the coil really does include “all” of the flux.

The form of eq. (138) is not very convenient for calculation if fast-Fourier transforms (FFTs) are used. In such an event, we can obtain the following equation by directly substituting for $\cos(\nu L/2)$ and $\sin(\nu L/2)$ and making use of the symmetry properties of Fourier transforms.

$$\begin{aligned} \int_I dz = & i \frac{b^{\pm} \ell M}{c} e^{\pm i\omega_1 t} k_{nm} \int_{-\infty}^{\infty} \left\{ \frac{W_{nm}(\nu)}{\mu^2 + \nu^2} \mu \sinh\left(\mu \frac{L}{2}\right) e^{i\nu \frac{L}{2}} + \cosh\left(\mu \frac{L}{2}\right) \right. \\ & \left. \times \nu \frac{[W_{nm}(\nu) - W_{nm}^*(\nu)]}{\mu^2 + \nu^2} e^{i\nu \frac{L}{2}} \right\} d\nu. \end{aligned} \quad (140)$$

We see from eqs. (139) and (140) that these integrals contain both normal and skew components in principle. Considerable care must be taken if eq. (140) is used with FFTs to ensure that aliasing and boundary discontinuities do not produce spurious values of the integral. In view of the complexity of eqs. (139) and (140) it may often be easier to integrate eq. (135) numerically. Finally, the contribution from the cosh term is 13% of the contribution of the cos term (see eqs. (140) and (139)) so if the sag is small, the contribution of eq. (139) can be neglected.

Now we treat the tangential component of the vibration considered above. The treatment will be similar to the treatment presented in section 4.6.1. By definition, eq. (99), the tangential component of the radial vibration only produces a z -dependent variation in the azimuthal angle θ which is given by

$$\theta(t, z) = \omega t + \frac{\tau^{\pm}}{Ac} Y(z) e^{\pm i\omega_1 t}, \quad (141)$$

where $Y(z)$ is given by eq. (130) and $\tau^+ = C_3 \sin(\vartheta)$ and $\tau^- = C_4 \sin(\vartheta)$. Following the procedures used to obtain eqs. (112) and (141) we obtain, after expanding $\exp[\theta(t, z)]$

$$\mathcal{E} = i \frac{d}{dt} \int_{-L/2}^{L/2} dz \sum_n e^{im\theta} \left[1 + \frac{in\tau^+}{Ac} Y(z) e^{-im\theta} \right] \sum_{m=0}^{\infty} \frac{n}{M} k_{nm}(z) \left(\frac{c}{a} \right)^m. \quad (142)$$

The result of carrying out the integration over z in eq. (142) is seen by inspection to lead to integrals identical to those given by eqs. (136)–(139). Hence the result is given by eqs. (115) and (116) plus the contributions from eq. (138) or eq. (139), where we remember that μ is now given by the solution to eq. (131) rather than eq. (97). The final results for the radial and tangential components are:

$$\begin{aligned} \mathcal{E} = & -\omega \sum_{m=-\infty}^{\infty} e^{im\theta} \sum_{n=0}^{\infty} \frac{n}{M} \left(\frac{c}{a} \right)^m \\ & \times \left\{ nK_n \delta_{m0} \delta_{nm} + \frac{2Mb^+}{c} (n \pm k) \left(\pi K_{nm}(\mu_1) + k \mathcal{J}_{nm} \left(\frac{L}{2} \right) \right) \frac{(-1)^{n-m} \sin(\pm k\pi)}{(n-m \pm k)\pi} \right\} \end{aligned} \quad (143)$$

$$\begin{aligned} \mathcal{E} = & -\omega \sum_{m=-\infty}^{\infty} e^{im\theta} \sum_{n=0}^{\infty} \frac{n}{M} \left(\frac{c}{a} \right)^m \\ & \times \left\{ nK_n \delta_{m0} \delta_{nm} + \frac{2in\tau^+}{c} (n \pm k) \left(\pi K_{nm}(\mu_1) + \ell \mathcal{J}_{nm} \left(\frac{L}{2} \right) \right) \frac{(-1)^{n-m} \sin(\pm k\pi)}{(n-m \pm k)\pi} \right\} \end{aligned} \quad (144)$$

where

$$\mathcal{J}_{nm} \left(\frac{L}{2} \right) = \int_{-L/2}^{L/2} \cosh(\mu_1 z) k_{nm}(z) dz \quad (145)$$

which may be obtained from eq. (138) or eq. (139).

The treatment of coil sag is a trivial modification of the treatment given in the previous section. Direct application of the boundary conditions to eq. (118) leads to

$$C_2 = -\frac{1}{2} L^2 C_4, \quad (146)$$

and

$$C_0 = \frac{1}{16} L^4 C_4. \quad (147)$$

The coefficient C_1 remains the same.

Hence the final result is similar to that derived in section 4.6.1 and eqs. (126) and (127) are also valid for the case where the bobbin ends are rigidly clamped as long as we use the appropriate values for the parameters b , τ , and C_p .

4.7. Effect of torsional vibrations

Torsional vibrations can arise from the rapid acceleration of the spindle as it starts, from the use of a stepping motor, or from a bearing catching. These vibrations also would be normally associated with an angular vibration which has already been discussed in section 4.4. As in the earlier discussion, we assume a rectangular coil that includes “all” of the flux. The differential equation describing the torsional vibration of a rigid beam, neglecting damping, is eq. [15]

$$\sigma I_z \frac{\partial^2 \theta}{\partial z^2} = \rho I_z \frac{\partial^2 \theta}{\partial t^2} \quad (148)$$

where σ is the modulus of rigidity or shear modulus, and I_z is the moment of inertia of the cross-sectional area about the z -axis. The general solution of eq. (148) is

$$\theta(z, t) = [\mathcal{T}_1 e^{i\mu z} + \mathcal{T}_2 e^{-i\mu z}] e^{i\omega_\tau t}, \quad (149)$$

where we adopt the \pm summation convention as before. The solution eq. (149) represents harmonic motion and hence a particular solution can be expanded in a Fourier series. The vibrational frequency is

$$\omega_\tau = \mu \sqrt{\sigma/\rho}. \quad (150)$$

As in the previous section, we will consider two classes of particular solutions which depend upon the specific boundary conditions we assume at the ends of the bobbin. (Recall that the origin of the z axis is in the center of the bobbin.) They are:

1. Sufficient elasticity and/or "slop" exists in the drive mechanism that we can consider both ends of the bobbin to be "free" once the oscillation is triggered. Hence

$$\frac{d\theta}{dz} = 0 \quad \text{at} \quad z = \pm L/2. \quad (151)$$

2. The drive end ($z = -L/2$) of the bobbin is assumed to be rigidly clamped. Hence

$$\begin{aligned} \theta(-L/2, t) &= 0, \\ \frac{d\theta}{dz}(+L/2, t) &= 0. \end{aligned} \quad (152)$$

Once again L is the length of the bobbin.

4.7.1. Class 1: Bobbin ends free

As in section 4.6.1, we see that the boundary conditions allow both the odd and the even cases, eq. (96). However, here the odd case will have the lowest frequency, given by eq. (150), with $\mu = \pi/L$. In general, $\mu = (2n-1)\pi/L$ with $n = 1, 2, \dots$ for the odd solutions. The even solutions will have $\mu = 2n\pi/L$ for $n = 1, 2, \dots$. Figs. 5a and 5b show the lowest two vibrational modes for the odd and even cases, respectively. The analysis of section 4.6.1, concerning the tangential component of the radial vibration is completely transferable to this case. In particular, we have that to first order in the expansion of eq. (112), namely eq. (113), the contribution from all the odd solutions of eq. (148) are zero (there will be very small contributions from the even order terms in the binomial expansion of eq. (112)). If we neglect the odd terms which integrate to zero, then in general the driving force generates a Fourier series of the form

$$\theta(z, t) = \omega t + \sum_{q=-\infty}^{\infty} \mathcal{T}_{2q} \cos(2q\mu z) e^{i2q\omega_\tau t}, \quad (153)$$

where we define \mathcal{T}_0 to be zero. We have immediately, on substituting eq. (153) into eq. (112) and following the steps leading to eq. (114), that

$$\mathcal{E} = i \frac{d}{dt} \sum_n e^{in\omega t} \sum_{m=0}^{\infty} \frac{n}{M} \left(\frac{c}{a}\right)^M \left\{ K_n \delta_{m0} + 2\pi i n \sum_{q=-\infty}^{\infty} \mathcal{T}_{2q} K_{nm}(2q\mu) e^{i2q\omega_\tau t} + \dots \right\} \quad (154)$$

where K_{nm} has been defined in eq. (108). If we integrate eq. (154) and then expand the result in a new Fourier series as we did in section 4.6, we obtain

$$Q = \sum_{n=-\infty}^{\infty} e^{in\theta} \sum_{m=0}^{\infty} \frac{n}{M} \left(\frac{c}{a}\right)^M \left\{ K_n \delta_{m0} \delta_{nm} + 2\pi i n \sum_{q=-\infty}^{\infty} \mathcal{T}_{2q} K_{nm}(2q\mu) \frac{(-1)^{n-m} \sin(k_q \pi)}{(n-m+k_q)\pi} \right\}, \quad (155)$$

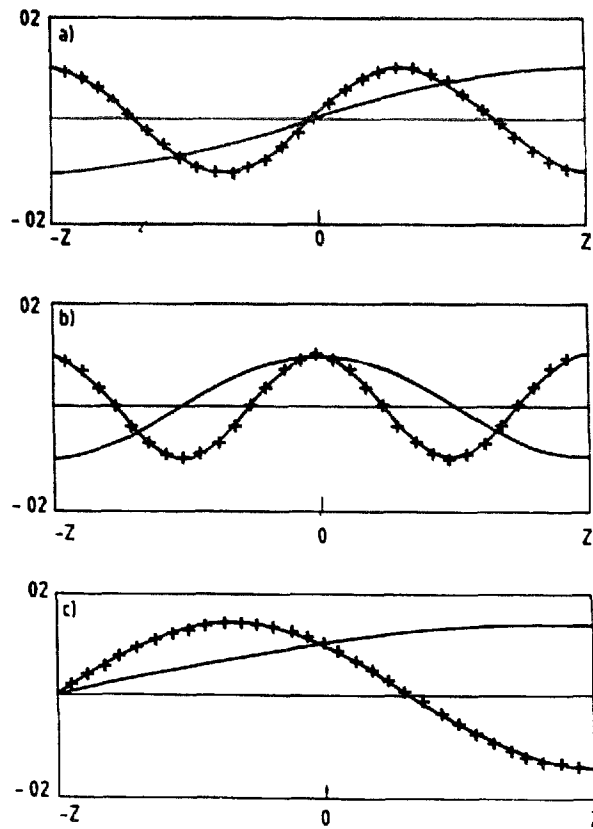


Fig. 5. (a) First two odd or sine-like torsional modes of vibration that satisfy the class 1 boundary conditions (ends of bobbin free) in section 4.7.1 (b) First two even or cosine-like modes that satisfy the class 1 boundary conditions (c) First two "mixed" modes of torsional vibration that satisfy the class 2 boundary conditions (drive end of bobbin "clamped") in section 4.7.2

where $k_q = 2q\omega_r/\omega$ and $\theta = \omega t$; $2q\mu$ and k_q are, of course, related by eq. (150). On carrying out the differentiation with respect to t in eq. (154) and re-expanding as before, we obtain

$$\mathcal{E} = -\omega \sum_{n=0}^{\infty} e^{im\theta} \sum_{m=0}^{\infty} \frac{n}{M} \left(\frac{c}{a} \right)^m \times \left\{ nK_n \delta_{m0} \delta_{nm} + 2\pi i n \sum_{q=-\infty}^{\infty} \mathcal{F}_{2q} K_{nm}(2q\mu)(n+k_q) \frac{(-1)^{n-m} \sin(k_q \pi)}{(n-m+k_q)\pi} \right\}. \quad (156)$$

As we saw in the previous section, integration of the EMF does not eliminate the effects of a torsional vibration, although it does reduce the amplitude by the factor $n/(n+k)$ as in the case of radial vibrations.

4.7.2. Class 2: Drive end of bobbin "clamped"

Substitution of the general solution eq. (149) into the equations for the boundary conditions eq. (152) leads to the following equations for the coefficients.

$$\begin{bmatrix} 0 \\ 0 \end{bmatrix} = \begin{bmatrix} e^{-i\mu \frac{L}{2}} & e^{i\mu \frac{L}{2}} \\ i\mu e^{i\mu \frac{L}{2}} & -i\mu e^{-i\mu \frac{L}{2}} \end{bmatrix} \begin{bmatrix} \mathcal{F}_1 \\ \mathcal{F}_2 \end{bmatrix} = \begin{bmatrix} \cos\left(\mu \frac{L}{2}\right) & -\sin\left(\mu \frac{L}{2}\right) \\ -\mu \sin\left(\mu \frac{L}{2}\right) & \mu \cos\left(\mu \frac{L}{2}\right) \end{bmatrix} \begin{bmatrix} \mathcal{E}_1 \\ \mathcal{E}_2 \end{bmatrix}. \quad (157)$$

These equations have a solution only when $\det[\dots] = 0$ which leads to the result $\mu = \pi/(2L)$. It is clear from eqs. (152) and (157) that both the even and the odd solutions are necessary to satisfy the boundary conditions of this class at all frequencies. The allowed frequencies are $q = 1, 3, 5, \dots, 2p - 1$ where $p = 1, 2, 3, \dots$. Furthermore, we see from eq. (157) that $\mathfrak{S}_2 = \mathfrak{S}_1 = \mathfrak{S}$ or $\mathcal{F}_2 = -\mathcal{F}_1^*$ which leads to $\mathcal{F}_{-q} = -\mathcal{F}_q^*$. Hence we can write the solution as (see fig. 5c)

$$\theta(z, t) = \omega t + \frac{1}{2} \sum_{q=1,3,5,\dots}^{\infty} \mathfrak{S}_q [\cos(q\mu z) + \sin(q\mu z)] e^{+i\varphi_q} e^{+iq\omega t} \tag{158}$$

where φ_q is the phase of the time dependent solution. From our previous discussion, we see that when we substitute eq. (158) into eq. (112) and expand as in eq. (114), the second term in [...] in eq. (158) integrates to zero and we are left with an equation identical to eq. (154); we must substitute \mathfrak{S} for \mathcal{F} and use the appropriate value for μ . The final results are

$$Q = \sum_{m=-\infty}^{\infty} e^{im\theta} \sum_{n=0}^{\infty} \frac{n}{M} \left(\frac{c}{a}\right)^M \times \left\{ K_n \delta_{m0} \delta_{nm} + \pi i n \sum_{q=1,3,5,\dots}^{\infty} \mathfrak{S}_q K_{nm}(q\mu) e^{+i\varphi_q} \frac{(-1)^{n-m} \sin(\pm k_q \pi)}{(n-m \pm k_q) \pi} \right\}, \tag{159}$$

for the integrated charge, and

$$\mathcal{E} = -\omega \sum_{m=-\infty}^{\infty} e^{im\theta} \sum_{n=0}^{\infty} \frac{n}{M} \left(\frac{c}{a}\right)^M \times \left\{ n K_n \delta_{m0} \delta_{nm} + \pi i n \sum_{q=1,3,5,\dots}^{\infty} \mathfrak{S}_q K_{nm}(q\mu) (n \pm k_q) e^{\pm i\varphi_q} \frac{(-1)^{n-m} \sin(\pm k_q \pi)}{(n-m \pm k_q) \pi} \right\} \tag{160}$$

for the EMF. All the comments in section 4.7.1 apply here. We note two significant differences, though. First, the vibrational frequency here is half that in the previous section. Secondly, now the vibration always has a component that looks like an angular vibration, as is easily seen from fig. 5c. As in the earlier cases, bucking coils would remove the strongest spurious harmonics if the torsional vibration affects the main coils and the bucking coils in the same way.

4.8. Effect of eccentricity of the coil

Errors in mounting the coil in the bobbin and/or errors in mounting of the bobbin on its bearings will usually lead to some eccentricity in the motion of the coil as it rotates. This eccentricity can affect the mean radius of the coil and introduce an apparent radial taper (see section 4.2). If the eccentricity is small it can be expressed as the truncated Fourier expansion of a decentered circle in polar coordinates (see section 4.11). The expansion has the form:

$$Y = a_0(z) + a_1(z) \cos(\vartheta) + b_1(z) \sin(\vartheta), \tag{161}$$

where the coefficients a and b must be linear functions of z if the bobbin is assumed to be perfectly cylindrical; we also assume that the origin of the coordinate system is at the center of the bobbin and the origin of ϑ is in the plane of the coil for a radial coil and in the plane of the bisector of a tangential coil. The coefficient $a_0(z) \equiv 0$ because we assume that we already know the mean radius c of the coil. The radius-of-eccentricity, \mathfrak{R} , and the phase angle φ are easily found to be

$$\mathfrak{R}(z) = \sqrt{[a_1(z)]^2 + [b_1(z)]^2}, \tag{162}$$

and

$$\varphi(z) = \tan^{-1} [b_1(z)/a_1(z)], \quad (163)$$

respectively.

The eccentricity can be resolved further into three components:

1. A correction to the mean radius of the coil δc .
2. An effective linear taper (see section 4.2).
3. A linear torsional error (see section 4.3).

Item 1 is clearly given by

$$\delta c = a_1(0) \cos(0) = a_1(0). \quad (164)$$

Because a and b are linear functions of z , items 2 and 3 are given by

$$b_1 = \frac{a_1(L/2) - a_1(-L/2)}{L} \quad (165)$$

$$\tau = \frac{b_1(L/2) - b_1(-L/2)}{L^2} \quad (166)$$

where the coefficients b_1 and τ are those defined in sections 4.2 and 4.3, respectively.

If the bobbin is aligned in the magnetic element then we see from sections 4.2 and 4.3 that, to first order in the expansions, neither a radial tilt ("effective taper") nor a torsional error affect the induced EMF when the coil includes "all" of the flux. Hence the only effect to first order of the eccentricity is to generate an error δc in the mean radius of the coil. To second order, we see from eq. (67) that there will be a term proportional to $\tau^2 Q_{nm}^{2p}(\infty)$. As we will see in section 4.9, there can be additional consequences in the case of the tangential coil geometry.

4.9. Errors specific to the tangential coil

Because the tangential coil has both arms active in generating the EMF, differences in the geometries of the arms influence the errors and spurious harmonics generated by the various vibrational modes and/or the eccentricity of the coil. Here we will deal with the effects resulting from differences in the radii of the two arms, a linear change in the tangential opening angle Ω , as well as radial vibrations and eccentricity.

4.9.1. z -dependent radial variations in the arms of the coil

Let us assume that the z -dependence of the radii of the two arms of the coil is given by

$$F_{\pm}(z) = c \pm \Delta c(z), \quad (167)$$

with

$$\pm \Delta c(z) = \pm \Delta c_0 + \sum_{p=1}^{\infty} b_p^{\pm} z^p. \quad (168)$$

The \pm corresponds to the arms at $\theta \pm \Omega/2$, respectively, b^{\pm} have the appropriate meaning. This definition implies that the mean value of r at $z = 0$ is c . From sections 3.2 and 4.2, we find that

$$\begin{aligned} \mathcal{E} = i \frac{d}{dt} \int_{-\infty}^{\infty} dz \sum_n \frac{n}{a} \left\{ e^{in(\theta + \Omega/2)} \sum_{m=0}^{\infty} k_{nm}(z) \int_0^{+\Delta c(z)} dr \left(\frac{r}{a} \right)^{M-1} \right. \\ \left. - e^{in(\theta - \Omega/2)} \sum_{m=0}^{\infty} k_{nm}(z) \int_0^{-\Delta c(z)} dr \left(\frac{r}{a} \right)^{M-1} \right\}. \end{aligned} \quad (169)$$

where $M = N + 2m$. If we perform the integration over r , we obtain

$$\mathcal{E} = i \frac{d}{dt} \sum_n n \int_{-\infty}^{\infty} dz \sum_{m=0}^{\infty} \frac{k_{nm}(z)}{M} \left\{ e^{im(\theta + \Omega/2)} \left(\frac{c + \Delta c + f^+}{a} \right)^M - e^{im(\theta - \Omega/2)} \left(\frac{c - \Delta c + f^-}{a} \right)^M \right\}, \quad (170)$$

where we have dropped the subscript on Δc for convenience and substituted

$$f^{\pm} = \sum_{p=1}^{\infty} h_p^{\pm} z^p.$$

Expansion of the trigonometric and trinomial functions up to second order as was done in 3.2 and 4.2 leads to

$$\begin{aligned} \mathcal{E} = & - \frac{d}{dt} \sum_{n,m=0}^{\infty} \frac{n}{M} \left(\frac{c}{a} \right)^M e^{im\theta} \int_{-\infty}^{\infty} dz k_{nm}(z) \\ & \times \left\{ \left[2 + M \frac{(f^+ + f^-)}{c} + \binom{M}{2} \frac{[2 \Delta c^2 + 2 \Delta c(f^+ - f^-) + f^{+2} + f^{-2}]}{c^2} \right] \sin\left(n \frac{\Omega}{2}\right) \right. \\ & \left. - i \left[M \frac{(2 \Delta c + f^+ - f^-)}{c} + \binom{M}{2} \frac{[2 \Delta c(f^+ + f^-) + f^{+2} - f^{-2}]}{c^2} \right] \cos\left(n \frac{\Omega}{2}\right) \right\}. \end{aligned} \quad (171)$$

If we assume for the moment that f^+ and f^- can be neglected, eq. (171) simplifies considerably. Since there is now no z -dependence, the integration over z can be done immediately and we obtain

$$\mathcal{E} = 2i\omega \sum_n N K_n \left(\frac{c}{a} \right)^N e^{in\theta} \left\{ \left[1 + \binom{N}{2} \left(\frac{\Delta c}{c} \right)^2 \right] \sin\left(n \frac{\Omega}{2}\right) + in \left(\frac{\Delta c}{c} \right) \cos\left(n \frac{\Omega}{2}\right) \right\}. \quad (172)$$

We have also carried out the differentiation with respect to t assuming $\theta = \omega t$, with ω constant. We see from eq. (172) that both normal and skew terms are generated by such an error. If, however, we choose $\Omega = \pi/n$, for the harmonic of interest (see section 3.2) then the cosine term in eq. (172) will vanish and the correction to the “normal” term is of the order of $(\Delta c/c)^2$.

In general, Δc will be explicitly a function of z and we cannot ignore the terms f^{\pm} . These terms are clearly of the same form as those in section 4.2 and the integral over z can be expressed in terms of moments $Q_{nm}^p(\infty)$ (eq. (61)).

We see from the above and from section 4.8 that if the coil is eccentrically mounted, then in general we will generate not only an error in the mean radius δc (eq. (164)), but also an error Δc (eq. (167)) as is readily seen from fig. 6. It is apparent from the figure and from eq. (161) that if the eccentricity is small, we can write

$$\Delta c = \frac{Y(\Omega/2) - Y(-\Omega/2)}{2} = b_1(0) \sin(\Omega/2). \quad (173)$$

The comments at the end of section 4.8 concerning longitudinal alignment clearly apply. As before, the effective taper introduced by the eccentricity integrates to zero if we include all of the flux.

4.9.2. Effect of a linear change in the tangential angle Ω

If the two arms of the coil are not exactly parallel, the tangential opening angle Ω will have a z -dependence. Let us assume that this z -dependence is linear and has the form

$$\Omega = \Omega_0 + \Omega' z \quad (174)$$

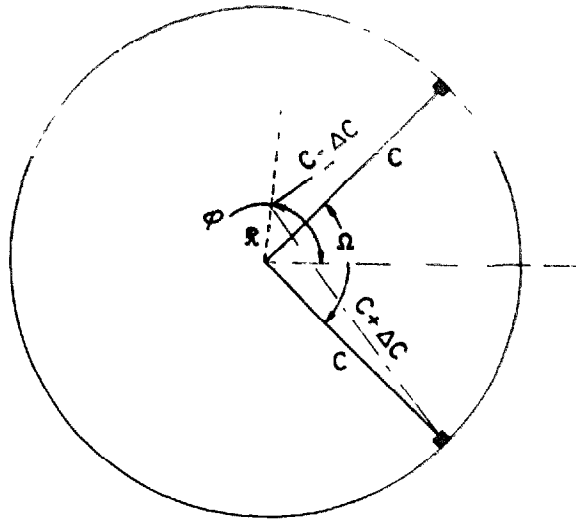


Fig. 6. Schematic representation of an eccentrically mounted tangential coil. The figure defines the relationship between "radius-of-eccentricity", R , the phase angle φ , discussed in section 4.8 and the radius errors Δc discussed in section 4.9.1

where $\Omega' = d\Omega/dz$ is constant. Then, from eqs. (34) and (45) we find that eq. (48) can be written in the form

$$\mathcal{E} = i \frac{d}{dt} \int dz \sum_n e^{in\theta} \{ e^{in(\Omega_0 + \Omega'z)/2} - e^{-in(\Omega_0 + \Omega'z)/2} \} \sum_m \frac{k_{nm}}{M} \left(\frac{c}{a} \right)^M. \quad (175)$$

Here we have integrated over r but not over z . If we assume that $|n\Omega'| \ll 1$ for all harmonics of interest, then we can expand the exponentials to obtain

$$\begin{aligned} \mathcal{E} = i \frac{d}{dt} \sum_n e^{in\theta} \int dz \left\{ e^{in\Omega_0/2} \left[1 + in \frac{\Omega'}{2} z - \frac{1}{2} \left(n \frac{\Omega'}{2} z \right)^2 + \dots \right] \right. \\ \left. - e^{-in\Omega_0/2} \left[1 - in \frac{\Omega'}{2} z - \frac{1}{2} \left(n \frac{\Omega'}{2} z \right)^2 + \dots \right] \right\} \sum_m \frac{k_{nm}}{M} \left(\frac{c}{a} \right)^M. \end{aligned} \quad (176)$$

This equation can be rearranged so that

$$\begin{aligned} \mathcal{E} = i \frac{d}{dt} \sum_n e^{in\theta} \int dz \left\{ [e^{in\Omega_0/2} - e^{-in\Omega_0/2}] + in \frac{\Omega'}{2} z [e^{in\Omega_0/2} - e^{-in\Omega_0/2}] \right. \\ \left. - \frac{1}{2} \left(n \frac{\Omega'}{2} z \right)^2 [e^{in\Omega_0/2} - e^{-in\Omega_0/2}] + \dots \right\} \sum_m \frac{k_{nm}}{M} \left(\frac{c}{a} \right)^M, \end{aligned} \quad (177)$$

which reduces to

$$\begin{aligned} \mathcal{E} = -2 \frac{d}{dt} \sum_n e^{in\theta} \sum_m \left(\frac{c}{a} \right)^M \int_{-L/2}^{L/2} dz \left\{ \sin \left(\frac{n\Omega}{2} \right) \left[1 - \frac{1}{2} \left(n \frac{\Omega'}{2} z \right)^2 + \dots \right] \right. \\ \left. + n \frac{\Omega'}{2} z \cos \left(\frac{n\Omega}{2} \right) \left[1 - \frac{1}{6} \left(n \frac{\Omega'}{2} z \right)^2 + \dots \right] \frac{k_{nm}}{M} \right\}. \end{aligned} \quad (178)$$

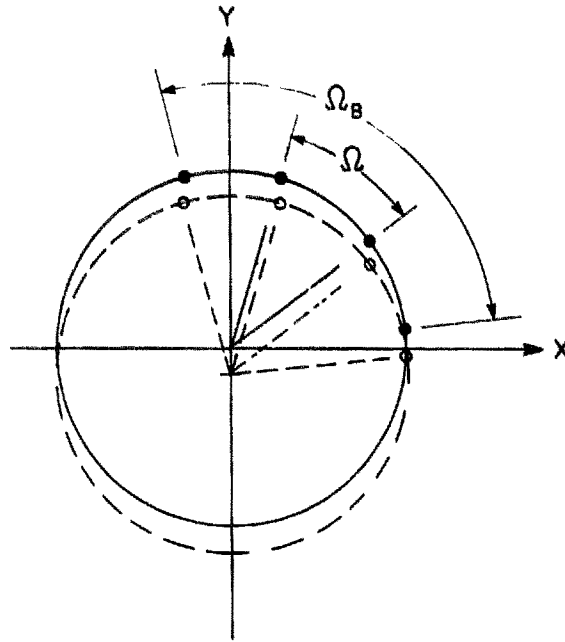


Fig. 7. Schematic representation of a tangential coil with opening angle Ω and its bucking coil with angle Ω_B showing the effect of coil sag (dashed circle).

The integral over z can be expressed in terms of functions Q_{nm}^p , eq. (61), with the result that

$$\mathcal{E} = -2 \frac{d}{dt} \sum_n e^{im\theta} \sum_m \frac{n}{M} \left(\frac{c}{a} \right)^M \sin \left(\frac{n\Omega}{2} \right) \left[K_n \delta_{m0} - \left(n \frac{\Omega'}{2} \right)^2 Q_{nm}^2 \left(\frac{L}{2} \right) + \dots \right], \quad (179)$$

where we have used the fact (see section 4.2) that the integral is zero for odd functions of z . Eq. (179) can be integrated directly with respect to t if desired. Again we obtain spurious harmonics of order $2m$ from such an error in the coil.

4.9.3. Effect of vibrations and coil sag

Vibrations are a more complicated problem for the tangential coil as is seen from fig. 7 because the vibration affects the two arms of the coil in slightly different ways. As coil sag is likely the most important “vibrational” mode, we will deal with it explicitly. The extension to general vibrations is straightforward. The result follows immediately if we substitute $\theta \Rightarrow \theta \pm \Omega/2$ and $\varphi \Rightarrow \pm \Omega/2$ into eq. (126), and eq. (127) for the radial and tangential components, respectively. We obtain after some manipulation

$$\begin{aligned} \mathcal{E} = & -2i\omega \sum_{m=-\infty}^{\infty} e^{im\theta} \sum_{n=0}^{\infty} \frac{n}{M} \left(\frac{c}{a} \right)^M \\ & \times \left\{ nK_n \sin \left(n \frac{\Omega}{2} \right) \delta_{nm} \delta_{m0} \pm iM(n \pm 1) \sin \left[(m \pm 1) \frac{\Omega}{2} \right] \sum_{p=0}^4 \frac{C_p}{c} Q_{nm}^p(\infty) \delta_{m, n \pm 1} \right\}, \end{aligned} \quad (180)$$

for the radial component, and

$$\begin{aligned} \mathcal{E} = & -2i\omega \sum_{m=-\infty}^{\infty} e^{im\theta} \sum_{n=0}^{\infty} \frac{n}{M} \left(\frac{c}{a} \right)^M \\ & \times \left\{ nK_n \sin \left(n \frac{\Omega}{2} \right) \delta_{m0} \delta_{nm} \pm in(n \pm 1) \sin \left[(m \pm 1) \frac{\Omega}{2} \right] \sum_{p=0}^4 \frac{C_p}{c} Q_{nm}^p(\infty) \delta_{m, n \pm 1} \right\}. \end{aligned} \quad (181)$$

for the tangential component. Unlike the radial coil, the tangential coil does not generate a spurious dipole component from a quadrupole because $|m| - 1 \neq 0$ in eqs. (180) and (181). We do, of course, obtain a spurious sextupole. Similarly, coil sag produces a spurious quadrupole from a dipole field.

4.10. Errors in the alignment of the bucking coils

There are several sources of error that will limit the effectiveness of the bucking coils. These are: an error in the angle between the coils, a torsional error between the coils, a z -dependent radial error and the effects of the finite sizes of the coils. We will deal first with an error in the angle.

From eq. (45), we can write eq. (49) as

$$\mathcal{E} = i \frac{d}{dt} \left\{ \sum_n \frac{n}{N} K_n \left(\frac{c_1}{a} \right)^N e^{in\theta} - \sum_n K_n \left[\frac{c_1}{c_2} \right]^N \left(\frac{c_2}{a} \right)^N e^{in(\theta + \delta\theta)} \right\}, \quad (182)$$

where $\delta\theta$ is the angular displacement between the coils. The definitions of the other symbols is the same as in section 3.3. Eq. (182) reduces to

$$\mathcal{E} = i \frac{d}{dt} \sum_n \frac{n}{N} K_n e^{in\theta} \left\{ \left(\frac{c_1}{a} \right)^N - \left[\frac{c_1}{c_2} \right]^N \left(\frac{c_2}{a} \right)^N e^{in\delta\theta} \right\} \quad (183)$$

If we assume that $\delta\theta \ll 1$ then we can expand the last exponential to obtain

$$\mathcal{E} = i \frac{d}{dt} \sum_n \frac{n}{N} K_n e^{in\theta} \left\{ \left(\frac{c_1}{a} \right)^N - \left[\frac{c_1}{c_2} \right]^N \left(\frac{c_2}{a} \right)^N \left(1 + in\delta\theta - \frac{n^2 \delta\theta^2}{2} + \dots \right) \right\}. \quad (184)$$

We see that the angular error leads to a skew component which is linear in $n\delta\theta$, and a normal component which is proportional to $n^2 \delta\theta^2 / 2$. Identical results are obtained from an analogous treatment of the tangential geometry.

A z -dependent radial error in the bucking coil will lead to components identical to those in section 4.2, scaled by $(c_1/c_2)^N$. Thus a radial error between the coils will lead to spurious harmonics of the same order of magnitude as if no bucking coils were present. Similar remarks apply to the tangential geometry, but in addition, the types of errors discussed in section 4.9 must also be included. It is seen that in general, it will be more difficult to obtain as high a bucking ratio with the tangential geometry as should be possible with the radial geometry. Thus very careful assembly of the bucking coils is essential!

Similarly, a torsional error of the bucking coil with respect to the main coil will lead to components identical to those in section 4.3, also scaled by $(c_1/c_2)^N$. As in section 4.3, if the system is symmetric and we integrate over "all" of the flux, there will be no first order effect. Similar results are obtained for the tangential geometry.

If rectangular, rather than circular coils are used, the finite size of the bucking coils will lead to similar effects as those discussed in section 4.1. If we substitute eq. (54) into eq. (183), we obtain

$$\begin{aligned} \mathcal{E} = i \frac{d}{dt} \sum_n \frac{n}{N} K_n e^{in\theta} & \left\{ \left(\frac{c_1}{a} \right)^N \left[1 + \frac{N(N-1)}{6} \left(\frac{\Delta r_1}{c_1} \right)^2 + \dots \right] \left(1 - \frac{n^2 \Delta\theta_1^2}{6} + \dots \right) \right. \\ & \left. - \left[\frac{c_1}{c_2} \right]^N \left(\frac{c_2}{a} \right)^N \left[1 + \frac{N(N-1)}{6} \left(\frac{\Delta r_2}{c_2} \right)^2 + \dots \right] \left(1 - \frac{n^2 \Delta\theta_2^2}{6} + \dots \right) \right\}. \end{aligned} \quad (185)$$

We see from eq. (185) that complete cancellation of the terms resulting from the finite size of the coil will only occur if $(\Delta r_2/c_2) = (\Delta r_1/c_1)$ and $\Delta\theta_1 = \Delta\theta_2$. In general it is difficult to arrange this, especially if one wants to use the turns ratio of the coils rather than an electronic network to get the factor $(c_1/c_2)^N$.

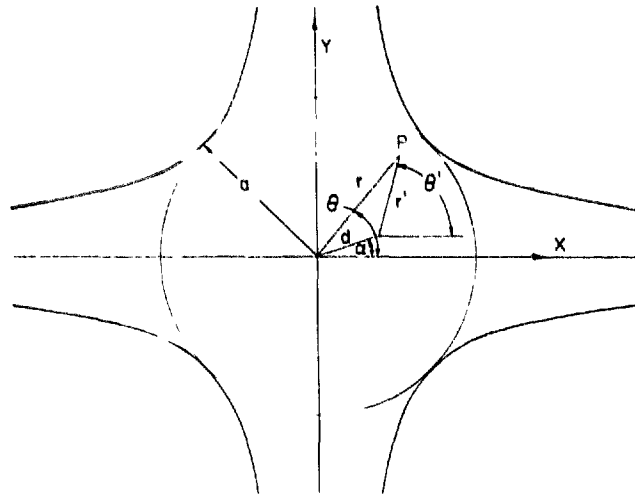


Fig. 8. Geometry of a radially decentered coil in a quadrupole element. The radial displacement d at angle α , the displaced radius r' and rotation angle θ' are defined with respect to the original coordinate system (r, θ) .

From eqs. (180) and (181) and fig. 7, we see that the bucking coils cannot cancel the dominant spurious components generated by coil sag (vibration coupling) because $\sin[(m \pm 1)\Omega/2] \neq C_n \sin[(m \pm 1)\Omega_B/2]$, where the bucking ratio C_n and the tangential angle of the bucking coil, Ω_B are defined in section 3.3. However, for the case of the dipole or quadrupole field, where $|m| - 1$ term is zero, C_n can be adjusted to remove the spurious quadrupole and sextupole terms respectively.

All of the above effects will limit the degree of cancellation of the “bucked-out” harmonic. Angular error is the most likely limiting factor. This is often alleviated by winding two bucking coils, each having an angular error $\pm\varphi$, and taking the appropriate linear combination to make the resultant angular error zero.

4.11. Radially misaligned apparatus.

A major potential source of harmonic contamination comes from the “feed-down” of higher harmonics due to a radial misalignment of the apparatus with respect to the magnetic center of the multipole lens. The geometry is shown in fig. 8. Although, we could derive the relationship between the displacement (d, α) , (r', θ') and (r, θ) using plane geometry, the same results can be obtained much more efficiently if we use complex algebra. Let us denote the vector (r, θ) in fig. 8 by z , and similarly (d, α) by z_d and (r', θ') by z' . Then, we have that

$$z^N = (z_d + z')^N = \sum_{l=0}^N \binom{N}{l} z_d^{N-l} z'^l \tag{186}$$

where

$$\binom{N}{l} = \frac{N!}{l!(N-l)!}, \tag{187}$$

the binomial coefficient. If we substitute the exponential form $z = r \exp(i\varphi)$ with φ replaced by $l\theta$, then eq. (186) can be written in the form

$$\left(\frac{r}{a}\right)^N e^{iN\theta} = \sum_{l=0}^N \binom{N}{l} \left(\frac{d}{a}\right)^{N-l} \left(\frac{r'}{a}\right)^l e^{i(N-l)\alpha} e^{il\theta'}, \tag{188}$$

where we have normalized to the aperture radius a . If we substitute eq. (188) into the expression for Φ #3, (eq. (21)), we obtain

$$\Phi(r', \theta', z) = \sum_n \sum_{l=0}^n \left(\frac{N}{|l|} \right) \left(\frac{d}{a} \right)^{N-|l|} \left(\frac{r'}{a} \right)^{|l|-1} e^{i(n-l)\alpha} e^{il\theta'} \sum_{m=0}^{\infty} k_{nm}(z) \left(\frac{r}{a} \right)^{2m}, \quad (189)$$

where we still have the factor $(r/a)^{2m}$ in the original coordinate system. The gradient of Φ in the new coordinates leads to

$$B_{\theta'} = -\frac{1}{r'} \frac{\partial \Phi}{\partial \theta'} = -\frac{1}{a} \sum_n \sum_{l=0}^n \left(\frac{N}{|l|} \right) \left(\frac{d}{a} \right)^{N-|l|} \left(\frac{r'}{a} \right)^{|l|-1} e^{i(n-l)\alpha} e^{il\theta'} \sum_{m=0}^{\infty} k_{nm}(z) \left(\frac{r}{a} \right)^{2m} \times \left\{ il + 2mr'd \sin(\theta' - \alpha) \left(\frac{r}{a} \right)^{-2} \right\}. \quad (190)$$

Here we have made use of the Pythagorean relation (see fig. 8)

$$r = (r'^2 + d^2 + 2r'd \cos(\theta' - \alpha))^{1/2}. \quad (191)$$

In general, eq. (190) leads to integrals that are extremely difficult, if not impossible to evaluate analytically. However, since the terms that originate from the misalignment have been assumed to be independent of z , we can integrate over z . From eqs. (31) and (33) we find by inspection that

$$B_{l_{\theta'}} = -\frac{i}{a} \sum_n K_n \sum_{l=0}^n l \left(\frac{N}{|l|} \right) \left(\frac{d}{a} \right)^{N-|l|} \left(\frac{r'}{a} \right)^{|l|-1} e^{i(n-l)\alpha} e^{il\theta'}, \quad (192)$$

whereas in eq. (35), all term with $m > 0$ vanish. The induced EMF can now be obtained from eqs. (34) and (38) by inspection, giving

$$\mathcal{E}_{l_{\theta'}} = i \frac{d}{dt} \sum_n K_n \sum_{l=0}^n \left(\frac{N}{|l|} \right) \left(\frac{d}{a} \right)^{N-|l|} \left(\frac{c}{a} \right)^{|l|} e^{i(n-l)\alpha} e^{il\theta'}. \quad (193)$$

We see that radial misalignment produces a complex spectrum of spurious harmonics feeding down from each real harmonic n . Table 1 shows how the coefficient

$$C = \left(\frac{N}{|l|} \right) \left(\frac{d}{a} \right)^{N-|l|} \quad (194)$$

varies as a function of l for selected values of n .

The table clearly shows that the fed-down harmonics of greatest importance are the ones nearest to their "parent". One might think that perfect alignment could be achieved by simply zeroing the dipole component $l = 1$. The situation is not so simple because radial vibrations, and, in particular coil sag, will also produce a dipole component which, in general, will lead to a small residual offset.

4.12. Non-linearity in the electronics

As final topics in our analysis of rotating coil mapping machines, we will look at the effects of two types of non-linearity in the electronics: (a) a simple quadratic non-linearity in the amplifiers, voltmeter

#3 The Fourier series, eq. (16) for example, can be written as

$$\Phi = \sum_{n=-\infty}^{\infty} U_n e^{in\theta} = U_0 + \sum_{n=1}^{\infty} [U_n e^{in\theta} + U_n^* e^{-in\theta}]$$

which justifies eq. (189)

Table 1
Values of C' for $(d/a) = 0.1$

l	n				
	2	3	4	6	10
1	0.2	0.03	0.004	6×10^{-5}	1×10^{-8}
2	1.0	0.3	0.06	0.0015	0.45×10^{-6}
3		1.0	0.4	0.02	12×10^{-6}
4			1.0	0.15	0.21×10^{-3}
5				0.6	2.5×10^{-3}
6				1.0	0.021
7					0.12
8					0.45
9					1.0
10					1.0

or integrator, and (b) an offset error which might occur in a V/f circuit of the type designed by Green et al. [7]. Let us assume in case (a) that the Fourier analysis program sees a signal of the form

$$\mathcal{V} = \mathcal{E} + b\mathcal{E}^2, \tag{195}$$

where b is a constant. For the sake of simplicity, let us also assume that \mathcal{E} is given by eq. (38), which if substituted into eq. (195) leads to

$$\begin{aligned} \mathcal{V} &= -\omega \sum_n K_n \left(\frac{c}{a}\right)^N e^{in\theta} + b \left\{ -\omega \sum_n K_n \left(\frac{c}{a}\right)^N e^{in\theta} \right\} \left\{ -\omega \sum_n K_n \left(\frac{c}{a}\right)^{|n|} e^{in\theta} \right\} \\ &= -\omega \sum_n K_n \left(\frac{c}{a}\right)^N e^{in\theta} + b \left\{ \omega^2 \sum_n \sum_n K_n K_n \left(\frac{c}{a}\right)^{N+|n|} e^{i(n+n)\theta} \right\}. \end{aligned} \tag{196}$$

We see that the non-linearity mixes all of the harmonics present in the magnetic field and produces a complete set of sum and difference “side-bands”, just as in amplitude modulation. (Remember: n and n range over both positive and negative numbers in the exponential form of the Fourier series.)

Finally, the effects of a zero-crossing offset, or “pole-zero” error, will be studied. Mathematically, we can model this effect as follows:

$$\mathcal{V} = \text{sign}(\mathcal{E})\{|\mathcal{E}| + a\}, \tag{197}$$

where the constant a , the offset error, will usually be very small. If we once again assume that \mathcal{E} is given by eq. (38), we can expand eq. (197) in a new Fourier series as was done in eqs. (70) and (71) of section 4.4. We obtain

$$c_m = \frac{1}{2\pi} \left\{ \int_{-\pi}^{\pi} -\omega K_n \left(\frac{c}{a}\right)^N e^{i(n-m)\theta} d\theta - \eta \int_{-\pi/\eta+\alpha}^{\alpha} a e^{-im\theta} d\theta + \eta \int_{\alpha}^{\pi/\eta+\alpha} a e^{-im\theta} d\theta \right\}, \tag{198}$$

where η is the periodicity of \mathcal{E} , usually the smallest value of n in the multipole field, and α is the phase – usually small – required to place the zero-crossing at the correct position. Here we have broken up the wave-form into η cycles because in each half-cycle a adds to or subtracts from \mathcal{E} , as indicated in eq. (197). The first term in eq. (198) becomes

$$-\omega K_n \left(\frac{c}{a}\right)^N \left[\frac{e^{i(n-m)\pi} - e^{-i(n-m)\pi}}{2\pi i(n-m)} \right] = -\omega K_n \left(\frac{c}{a}\right)^N \delta_{mn}, \tag{199}$$

so we recover the original spectrum. The second and third terms in eq. (198) reduce to

$$\begin{aligned} & i \frac{\eta a}{2m\pi} [e^{im(\pi/\eta - \alpha)} - e^{-im\alpha} + e^{-im(\pi/\eta + \alpha)} - e^{im\alpha}] \\ &= i \frac{\eta a}{2m\pi} [e^{im\pi/\eta} + e^{-im\pi/\eta} - 2] e^{-im\alpha} - i \frac{\eta a}{m\pi} \left[\cos\left(\frac{m\pi}{\eta}\right) - 1 \right] e^{-im\alpha}. \end{aligned} \quad (200)$$

For eq. (200) to have the correct periodicity, m must be a multiple of η so m must be replaced by ηm . If we substitute ηm for m in eq. (200), it is easy to show that the expression in [] in eq. (200) is zero unless m is an odd integer. Hence we obtain the final expression for the distorted spectrum

$$\mathcal{V} = -\omega \sum_{m=-\infty}^{\infty} K_m \left(\frac{c}{a}\right)^m e^{im\theta} \delta_{mn} - 2 \frac{ia}{\pi} \sum_{m=-\infty}^{\infty} \frac{1}{m} e^{-i\eta m\alpha} e^{i\eta m\theta} \delta_{m \text{ odd}}. \quad (201)$$

As expected, we recover the original spectrum plus an infinite series of spurious harmonics that are built on the fundamental frequency $n = \eta$. Furthermore, the amplitude of the fundamental is no longer the original, but is changed by an amount $2a/\pi$. The spurious harmonics are the allowed harmonics given by eq. (14) and decrease in amplitude as $1/m$. Finally, although it may appear that the spurious terms are skew, this is not the case. From fig. 1, we see that the coordinate system is aligned such that K_n is imaginary, that is $\mathcal{E} \propto \sin(n\theta)$. The spurious terms also possess this property.

5. Conclusions

In this article, we have derived expressions for the EMF induced in the rotating coil of a magnetometer designed to measure the fields of dipole, quadrupole and higher order multipole magnets used in ion-optics and particle accelerators. A complete three-dimensional magnetic field expansion was used throughout. A comprehensive discussion of the factors that limit the precision and accuracy of the measurement of the harmonic structure of the magnetic field has been presented. Vibration, coil sag and misalignment of the apparatus have been identified as potential major problems associated with these measurements, although the use of integration and “bucking coils” go a long way towards alleviating these problems. Clearly, precise and accurate measurements of the amplitude of the fundamental and the usually very weak, but important, higher harmonics in these elements is a demanding task. It is hoped that this article will aid in the understanding of those factors that make these measurements so difficult and will aid in the design of better instruments as well as in understanding the results obtained.

Acknowledgements

It is a pleasure to thank Dr. Graham Lee-Whiting for many helpful discussions, Dr. G.C. Ball for his careful proofreading of the manuscript and Margaret Carey for her assistance in formatting and printing the manuscript. The algebraic code Derive has been used to check parts of this document. The manuscript was typed with Chiwriter.

References

- [1] G.E. Lee-Whiting, Nucl. Instr. and Meth. 82 (1970) 157.
- [2] J. Cobb and R. Cole, Spectroscopy of Quadrupole Magnets. Int. Symposium on Magnet Technology, Stanford, 1965.
- [3] K. Halbach, Nucl. Instr. and Meth. 74 (1969) 147.
- [4] K. Halbach, Nucl. Instr. and Meth. 78 (1970) 185.
- [5] K. Halbach, Nucl. Instr. and Meth. 119 (1974) 329.

- [6] W.V. Hassenzahl, An Algorithm for Eliminating the Duodecapole Component in Quadrupole Magnets, Fourth Int. Conf. on Magnet Tech., Upton, N.Y., 1972, ed. Y. Winterbottom (US Dept. of Com.) p. 469.
- [7] M.I. Green, P.J. Barale, D.H. Nelson and D.A. Van Dyke, Proc. of the Part. Accel. Conf., Washington D.C. (1987), eds. E.R. Lindstrom and L.S. Taylor, IEEE Cat. # 87CH2387-9, p. 1573.
- [8] J. Herrera, H. Kirk, A. Prodell, E. Willen, 12th Int. Conf. High-Energy Accel., FNAL, Aug. (1983), eds. F.T. Page and R. Donaldson (US Dept. of Com.) p. 563.
- [9] J.D. Jackson, *Classical Electrodynamics* (Wiley, 1962);
W.K.H. Panofsky and M. Phillips, *Classical Electricity and Magnetism* (Addison-Wesley, 1961).
- [10] J. Mathews and R.L. Walker, *Mathematical Methods of Physics* (Benjamin, New York, 1964);
A. Erdélyi, *Tables of Integral Transforms* (McGraw-Hill, New York, 1954).
- [11] G.E. Lee-Whiting, private communication.
- [12] K. Halbach, private communication.
- [13] P.M. Morse, *Vibration and Sound* (McGraw-Hill, New York, 1946).
- [14] J.L. Synge and B.A. Griffith, *Principles of Mechanics* (McGraw-Hill, Toronto, 1959).
- [15] L.D. Landau and E.M. Lifshitz, *Theory of Elasticity* (Addison-Wesley, Reading Massachusetts, 1959).